NASA SP-8011

NASA
SPACE VEHICLE
DESIGN CRITERIA
(ENVIRONMENT)

MODELS OF VENUS ATMOSPHERE (1972)

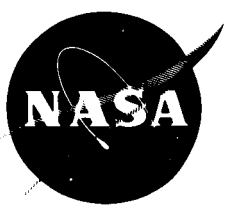

REVISED
SEPTEMBER 1972

NATIONAL AERONAUTICS AND SPACE ADMINISTRATION

FOREWORD

NASA experience has indicated a need for uniform criteria for the design of space vehicles. Accordingly, criteria have been developed in the following areas of technology:

Environment
Structures
Guidance and Control
Chemical Propulsion

Individual components of this work are issued as separate monographs as soon as they are completed. A list of all monographs published in this series can be found on the last pages of this monograph.

These monographs are to be regarded as guides to design and not as NASA requirements, except as may be specified in formal project specifications. It is expected, however, that the monographs will be used to develop requirements for specific projects and be cited as the applicable documents in mission studies, or in contracts for the design and development of space vehicle systems.

This monograph was prepared for NASA under the cognizance of the NASA Goddard Space Flight Center with Scott A. Mills as program coordinator. Principal authors were Richard B. Noll of Aerospace Systems, Inc. and Dr. Michael B. McElroy of Harvard University. The Technical Director was Mr. John Zvara of Aerospace Systems, Inc.

An ad hoc committee at GSFC, chaired by Dr. S. J. Bauer, provided technical guidance in preparation of this monograph. Committee members were Dr. J. R. Herman and Mr. J. E. Ainsworth of GSFC.

Comments concerning the technical content of these monographs will be welcomed by the National Aeronautics and Space Administration, Goddard Space Flight Center, Systems Reliability Directorate, Greenbelt, Maryland 20771.

September 1972

CONTENTS

MODELS OF VENUS ATMOSPHERE (1972)

1. INTRODUCTION

Design and mission planning for space vehicles which are to orbit the planet Venus, enter its atmosphere, or land on the surface require the best available information on its atmosphere. The atmosphere affects the orbital lifetime, the flight dynamics of the vehicle along its trajectory or flight path, and the performance of the vehicle and its major subsystems (ref. 1). For design of experiments, knowledge of the Venus atmosphere is required to select instrumentation and establish the range of measurements within suitable limits.

Quantitative data for the Venus atmosphere have been obtained from Earth-based observations and from spacecraft which have entered the Venus atmosphere or passed within several planetary radii of the planet. These data have been used in conjunction with existing theories of planetary atmospheres to predict other characteristics of the Venus atmosphere (ref. 2). Because of limited observational data, extrapolation within the limits of applicable theory was necessary to establish reasonably complete model atmospheres for this monograph. Earth-based observations have generally provided information on the composition, temperature, and optical properties of Venus, whereas spacecraft measurements have yielded data on composition, temperature, pressure, density, and atmospheric structure.

The models herein provide the temperature, pressure, and density profiles required to perform basic aerodynamic analyses. The profiles are supplemented by computed values of viscosity, specific heat, and speed of sound. These ambient values and the calculated aerodynamic forces influence flight dynamics and space vehicle design, i.e., configuration, size, strength, and materials. Other characteristics are inferred from the measured data that influence the design of the space vehicle and its subsystems. For example, electron densities of the ionosphere and the plasma characteristics in the region of the solar wind may dictate requirements for electromagnetic shielding. Also, opacity of the atmosphere can constrain the design of landed solar power systems and influence the performance of communications equipment, and clouds may adversely affect performance of experiments.

This monograph provides a set of engineering models for the Venus atmosphere on the basis of theory and measured data available in January 1972. It replaces NASA SP-8011 of December 1968 (ref. 3) which was based on data available at that time. Additional data from U.S. and U.S.S.R. space exploration have narrowed considerably the range of parameters in the lower atmosphere in comparison to the 1968 monograph. The six model atmospheres developed herein include a nominal model and five other models which encompass reasonable extremes for molecular mass, solar activity, and exospheric temperature.

Design criteria monographs on other planets, Earth environments, and space technology are listed in the last pages of this monograph.

2. STATE OF THE ART

2.1 Source Data

Knowledge of Venus has grown rapidly in recent years. The advance has proceeded on a variety of fronts. Radio and radar astronomy played a major role and provided the first indications that the surface temperature was exceedingly large. The evidence, however, was not generally accepted prior to 1967 and the successful flights of Mariner 5 and Venera 4. It was difficult to account physically for the observed radio brightness and a variety of more or less esoteric models were devised to account for the radio data using nonthermal emission mechanisms. A variety of interpretations of the data led to widely differing atmospheric models (refs. 4 to 8). Even the models in reference 3, which included data from Mariner 5 and Venera 4, reflected considerable uncertainty in values of the planetary radius, surface pressure, and surface temperatures. The uncertainties have been reduced significantly since 1967. Before presenting the updated models, the sources of data are reviewed for the various parameters which characterize the atmosphere of Venus.

2.1.1 Earth-Based Measurements

2.1.1.1 Optical

Optical observations of Venus by ground-based telescopes established the existence of a dense atmosphere, identified its major constituent, established the existence of extensive cloud cover, and determined the optical size of the planet.

Photographs taken in ultraviolet light reveal variable patterns which are interpreted as high altitude clouds (ref. 9). In yellow or red light, markings are not discernible except on rare occasions. The cloud pattern appears to move across the planetary disc in retrograde motion, corresponding to a rotation period of 4 to 5 days (sec. 2.2.2.5). The photographic evidence is interpreted as showing multiple cloud layers, that is, an upper cloud layer opaque to ultraviolet light and transparent to visible and near-infrared solar radiation which is reflected from a featureless lower cloud layer (ref. 10).

Venus, viewed under visible or near-infrared light, presents a disc which is optically larger than the actual solid planet because of the opaque layer of clouds. Measurements taken during occultation of the star Regulus by Venus in 1959 (refs. 11 and 12) resulted in a value of 6169 ±2 km for the occultation height (about 40 km above the visible cloud layer). A mean value for the optical radius of 6120±8 km was determined from the occultation result and the results of numerous other studies (refs. 10 and 13). More recent measurements yielded 6100 km in red and near-infrared light and 6145 km in ultraviolet (ref. 14) which indicated the existence of two distinct layers.

Spectroscopic measurements in the near-infrared bands have been used to determine the basic constituents of the Venus atmosphere (refs. 15 and 16). These measurements have affirmed that carbon dioxide (CO_2) is the dominant atmospheric constituent. Other gases

identified include hydrogen chloride (HCl), hydrogen fluoride (HF), carbon monoxide (CO), and oxygen (O_2). Water vapor was also tentatively identified by spectral observations but there is lack of agreement as to the amount (ref. 17). However, it is acknowledged that water is a minor constituent. Its abundance may be variable on the basis of Earth-based spectroscopy.

High-altitude aircraft and balloons have been used to carry spectroscopic instrumentation above the bulk of the Earth's atmosphere with resultant reduction in the errors and attenuation caused by the atmospheric constituents, particularly water vapor. Interferometer observations made from a Convair 990 jet aircraft at altitudes of 12 to 13 km revealed a very low but finite mixing ratio of H_2O/CO_2 (ref. 14). These data were confirmed by similar measurements obtained from balloon flights.

Results of interferometer spectrometer measurements of the reflection spectra of Venus are shown in figure 1. Reflection spectra have been used to investigate the constituents of the Venus cloud layers. The variations in albedo, i.e., the measure of the radiation reflected by a given surface, at the various wavelengths were associated with known spectra of chemical elements, compounds, and gaseous mixtures. For example, comparison of spectra obtained for the Venus upper cloud layer and those obtained from laboratory experiments led to an identification of partially-hydrated ferrous chloride as a possible constituent of the Venus clouds (ref. 14). The identification is not generally accepted by planetary scientists, however.

Studies of the polarization of light reflected by Venus provide a valuable source of information on the properties of the cloud particles. Polarization measurements reported in references 18 and 19 were compared to theoretical calculations in reference 20. Particle shape and dispersion in the clouds were determined, and it was concluded that the cloud particles are most likely liquid. The refractive index of the cloud layer was found to be 1.46±.02 in ultraviolet light with a decrease to 1.43±.02 in the near-infrared region. The upper limit of the refractive index recently has been revised to 1.44±.02 at a wavelength of 0.55μm. These results helped to eliminate a number of potential cloud constituents. In particular, pure water or ice, a mixture of dust and water, or a mixture of mercury compounds failed to satisfy constraints imposed by the polarization data.

Polarization measurements were also used to estimate the atmospheric pressure near the top of the reflecting cloud layer (refs. 20 and 21). Computations for polarized light at ultraviolet wavelengths indicated pressures near the cloud top of about .050 atm (ref. 20). The analysis implied that either the reflecting cloud was located high in the stratosphere or that a second cloud layer was located in this region and the pressures derived from the ultraviolet studies referred to a region somewhere between the high-altitude cloud layer and the principal cloud layer.

2.1.1.2 Radio Astronomy

Measurements on the time delay of radar echoes from Venus can be analyzed in conjunction with astronomical and orbital data for Venus to obtain values for the mean equatorial radius

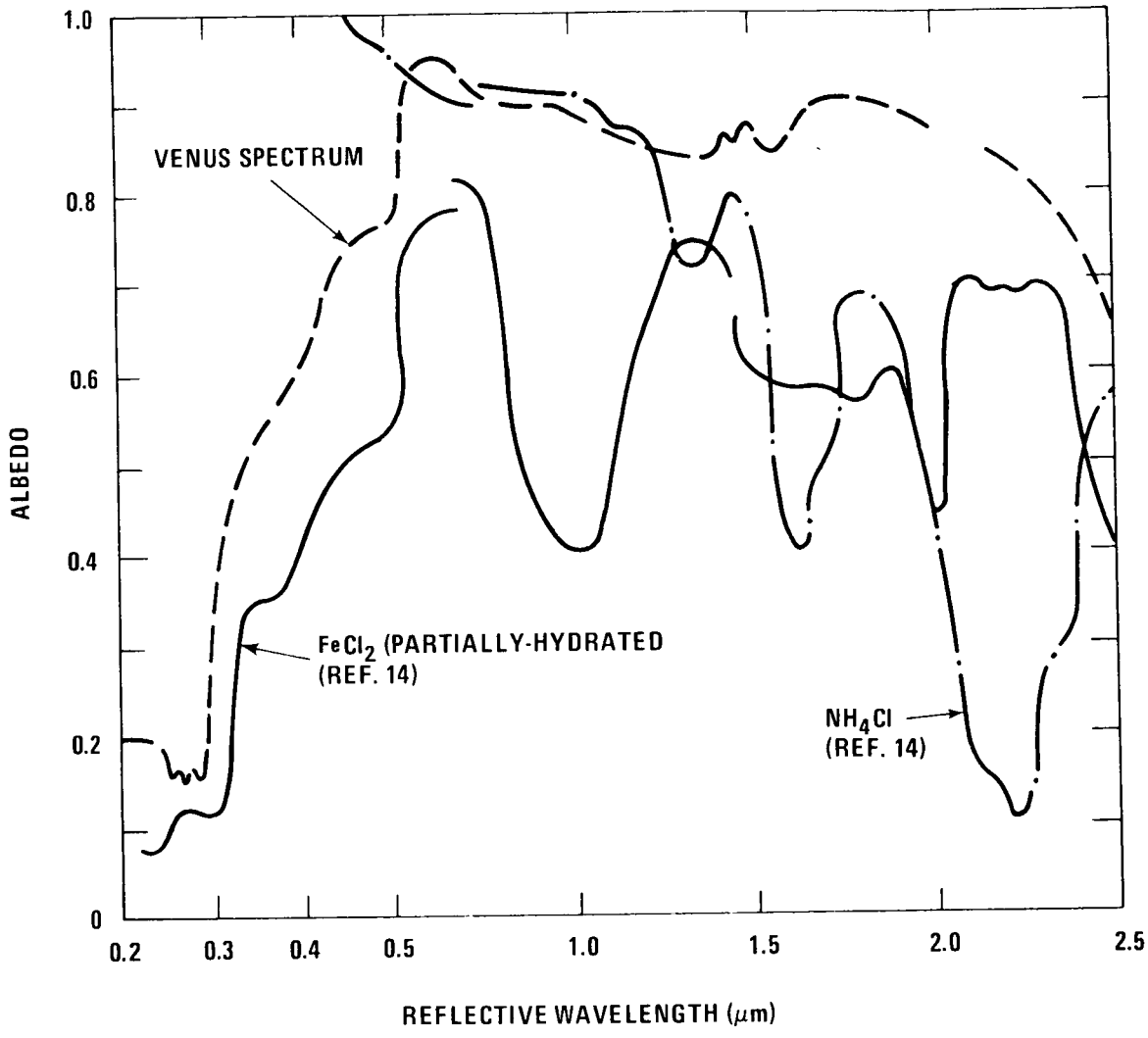

Figure 1.—Reflective spectrum of Venus.

(ref. 22). From the encounter of the Mariner 5 spacecraft with Venus it was possible to determine very accurately the position and velocity of the center of mass of Venus as well as its mass. The improved data were employed to compute a mean value for the planetary radius of 6053.7±2.2 km (ref. 23). Most recent data indicate a mean equatorial radius of 6050±0.5 with some evidence of topographic relief (ref. 24). Numerous values of radius are summarized in table 1.

Radar measurements are used to define the shape of the planet and to investigate the topography. Results indicate that the equatorial cross-section of the planet is an ellipse with the difference in semi-axes equal to 1.1±0.35 km (ref. 27). Surface height variations, detected by radar measurements, did not exceed 3 to 4 km (ref. 24).

TABLE 1

RADIUS OF VENUS

Radius (km)	Year of Publication	Reference
6057 ± 55	1965	25
6056 ± 1.2	1967	26
6048 ± 1	1968	26
6052 ± 2.0	1968	26
6053.7 ± 2.2	1968	23
6050 ± 5	1968	22
6050 ± 0.5	1972	24

Radio telescopes have been used to study the microwave emission spectrum of Venus and the data have been analyzed to determine the brightness temperature as a function of wavelength. Data reported in references 28, 29, and 30 indicate that Venus has a surface temperature of about 700K. Measurements at short radio wavelengths indicate a cool atmosphere with high opacity. The most accurate data are in the wavelength range of 2 mm to 21 cm. Microwave emission results are shown in figure 2. The opacity of the atmosphere is clearly indicated by the low brightness temperatures measured below 3 cm. Comparison of the observed spectra with analytic models shows that the opacity can be attributed to a high percentage of CO_2 in the atmosphere and 0.65±0.35% water vapor (ref. 29). Other results of this model indicate that any possible isothermal layer near the surface cannot be thicker than 4 km, that the radius is 6049.5±3 km, the surface temperature is 770±25K, and the surface pressure is 95±20 atm.

Radio interferometer measurements have been made to determine the temperature distribution of Venus (refs. 30 and 31). Results indicate that no large-scale differences in the surface temperature greater than 25K exist; in particular, the mean equatorial temperature is the same as that at the poles within 25K.

2.1.2 Spacecraft

2.1.2.1 Mariner 2

Mariner 2 passed within 34,751 km of the center of Venus in December 1962 (ref. 10). The spacecraft was equipped with a microwave radiometer and an infrared radiometer. The microwave radiometer used two channels, one to detect emissions at 1.35 cm which was sensitive to water vapor and the other at 1.9 cm which was relatively unaffected by water vapor so its detected emissions were expected to originate deeper in the atmosphere. Scans

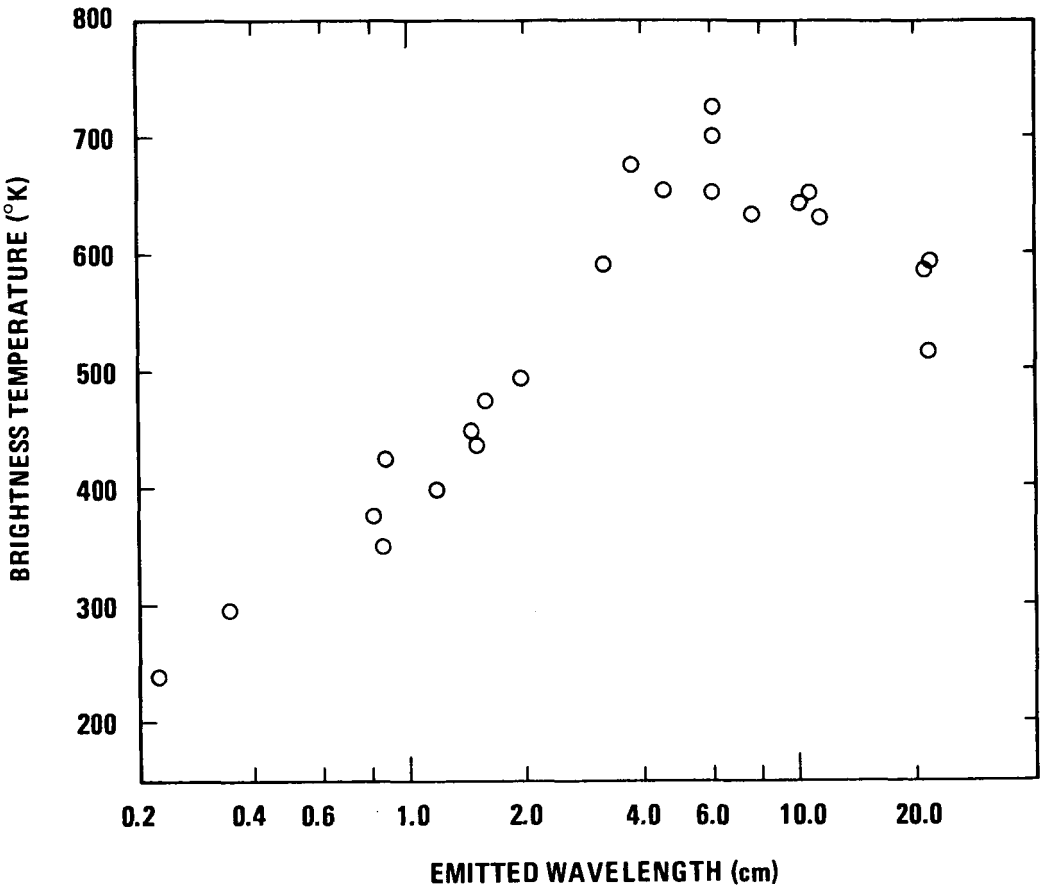

Figure 2.–Microwave spectrum of Venus (radio brightness) (ref. 29).

of the day and night sides and the terminator region showed no significant differences between the day and night sides of Venus. Highest temperatures were found along the terminator. Maximum brightness temperature recorded along the terminator was 590K±5% (ref. 32). The edges were observed to be cooler than the center of the planet; this was construed as a limb-darkening effect. Differences in the 1.35 and 1.9 cm data indicated the possibility of very low amounts of water vapor in the Venus atmosphere.

The infrared radiometer was sensitive to wavelengths of 8.4 and 10.4 μm which penetrate water vapor but not clouds. A temperature gradient detected across the planet was interpreted as a limb-darkening effect. The temperature was observed to decrease by approximately 20K between the central region (estimated at 240K) and the limbs (ref. 33). The similarity of the results at both wavelengths indicated that cloud temperatures had been measured and that the clouds were optically thick at both wavelengths.

2.1.2.2 Venera 4

The U.S.S.R. spacecraft Venera 4 entered the atmosphere on the night side of Venus on 18 October 1967 and performed measurements to determine composition, temperature, pres-

sure, and density. Initial reports claimed that the spacecraft had landed on the surface of Venus because calculations of the descent distance based on the measured parameters was in agreement with a value of 28 km obtained from a radio altimeter at the time of parachute deployment. Thus, the final measured value of temperature was considered to be the surface value in subsequent investigations (refs. 34 through 38). However, comparison with Mariner 5 data revealed a serious discrepancy. It was shown that transmission from Venera 4 ended when the spacecraft was still approximately 20 km above the mean planetary surface indicated by Earth-based radar. Either the radar data were in error, or Venus had local elevations of 20 km, or Venera 4 did not in fact reach the planetary surface (refs. 3, 41, 42, and 43). Subsequently, it was reported (refs. 39 and 40) that routine periodic modulation of the radio altimeter led to a faulty reading. An actual altitude reading in the 50 to 60 km range above the mean surface level was misconstrued as 28 km. Data transmission actually had been interrupted at about 26 km above the surface. The calculated rate of descent varied from 10 to 11 m/sec after parachute deployment to 2.5 to 3 m/sec at the interruption of data transmission.

Venera 4 was equipped with eleven gas analyzers to determine the composition of the Venus atmosphere. The analyzers were designed to detect CO_2, inert gases, O_2 and H_2O (refs. 44 and 45). Measurements were taken immediately after parachute deployment at a pressure of .7 atm and again when the pressure had increased to 2 atm. The data revealed that the major constituent is CO_2, accounting for 90±10% of the atmosphere and probably exceeding 90%. Other results reported included:

O_2	$>$ .4% but $<$ 1.6% (probably $\sim$ 1%)
N_2 and other inert gases	$<$ 7% (probably $<$ 2.5%)
H_2O	from 1 to 8 mg/liter

Atmospheric temperature, pressure, and density were measured with a resistance thermometer, an aneroid manometer, and a gas densitometer, respectively. Temperature was measured throughout the flight until termination at an altitude of 26 km and ranged from 304 to 544K (refs. 34, 46, and 47). Pressure was measured until it went off scale at 35 km (refs. 34, 38, and 42). Its range was from 0.7 atm to 7.5 atm. Density ranged between 1.4×10^{-3} and 1.2×10^{-2} g/cm^3. The densitometer went off scale at about 30 km (refs. 34, 38, 46, and 47). The temperature, pressure and density profiles are shown in figure 3 as a function of altitude above the mean surface. The temperature profile was determined to be basically adiabatic and the corresponding pressure profile could be determined analytically with the equations for hydrostatics and for quasi-uniform parachute descent (refs. 34, 38, and 42). The density profile (fig. 3) was felt to be in error between 34 and 43 km because the measured temperature and pressure data gave no indication of the non-monotonic nature of the profile in these altitudes (refs. 46 and 47). Possible errors in the densitometer readings are discussed in reference 47. As a result, a theoretical density profile was developed on the basis of the equation of state. This profile closely matched the measured profile except for the questionable region (refs. 34, 38, and 42).

Analyses of Venera 4 data revealed that the descent of the spacecraft was smooth and that the limiting value for convective currents in the atmosphere was 1.0 to 1.5 m/sec.

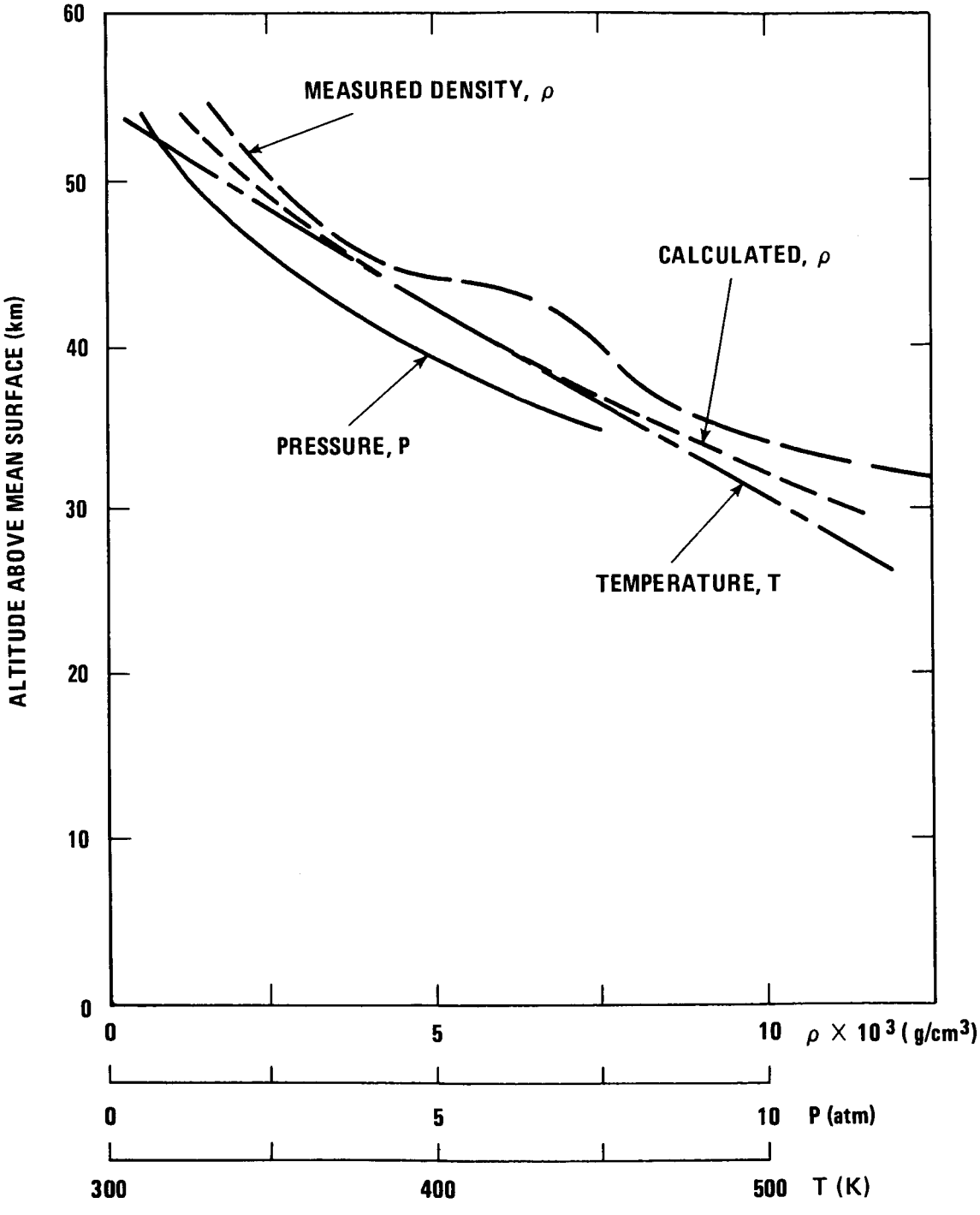

Figure 3.—Venera 4 measured data (refs. 34, 38 and 42).

Venera 4 measurements were compared to the equation of state and the variation of the partial water vapor pressure as a function of temperature. With the measured water vapor content of .5% and 1% as boundary values, it was determined that the lower boundary of a possible cloud layer was at an altitude of about 60 km. Also, if the clouds were formed by condensation, they consisted of ice crystals or supercooled water (refs. 34, 38, and 42). The thickness of the cloud layer was calculated to be 5 to 10 km. However, the validity of both the H_2O and O_2 measurements have been challenged in the subsequent literature because the stated abundances are not consistent with values inferred from ground-based spectroscopy.

2.1.2.3 Mariner 5

On October 19, 1967, the day after the flight of Venera 4 terminated, the Mariner 5 spacecraft encountered Venus at an altitude of less than one planetary radius. The trajectory, as viewed from Earth, passed almost diametrically behind the center of Venus. Two independent radio propagation experiments were conducted during the occultation of Mariner 5. One used a 2297 MHz (S-band) radio signal transmitted by the spacecraft (refs. 48 and 49). The other employed two harmonically-related frequencies, 49.8 and 423.3 MHz, which were transmitted from Earth to the spacecraft (refs. 49 and 50). The S-band experiment measured the refraction of the radio signal by the charged particles of the upper atmosphere and by the electrically-neutral gases that constitute the lower atmosphere. The refraction produced changes in the frequency phase and amplitude of the signal. In addition, the amplitude was affected by defocusing and absorption in the lower atmosphere. The dual frequency experiment provided Doppler and amplitude data of two harmonically-related frequencies as the signals passed through the ionosphere and neutral atmosphere of Venus. The locations where the radio beams of the two experiments probed the atmosphere are shown in figure 4. The spacecraft began occultation on the night side and emerged on the day side of the planet (ref. 50).

Besides the radio experiments, an ultraviolet (UV) photometer produced Lyman-alpha measurements of the distribution of radiating hydrogen atoms in the upper atmosphere on both the day and night sides of Venus (refs. 51 and 52).

High quality, two-way tracking data were used to calculate the orbital characteristics of Mariner 5. Perturbation analyses were conducted to determine the effects of Venus on the orbit so that the accuracy of the distance of the spacecraft from the center of Venus was known to high precision (ref. 48). Therefore, Mariner 5 data was determined relative to the planet center.

Data from the dual frequency experiments were converted to yield electron densities. Ionization profiles shown in figure 5 extend beyond an altitude of 1000 km on the night side and terminate in a plasmapause near 500 km on the day side. Both day-and night-side profiles peaked at about 140 km with the day-side density reaching a peak value of about 5.5×10^5 electrons/cm^3. The maximum density on the night side was about 2×10^4 electrons/cm^3 (ref. 50). Differences between the day side and night side and residual electron-content data showed that the distribution of ionization was not symmetric and indi-

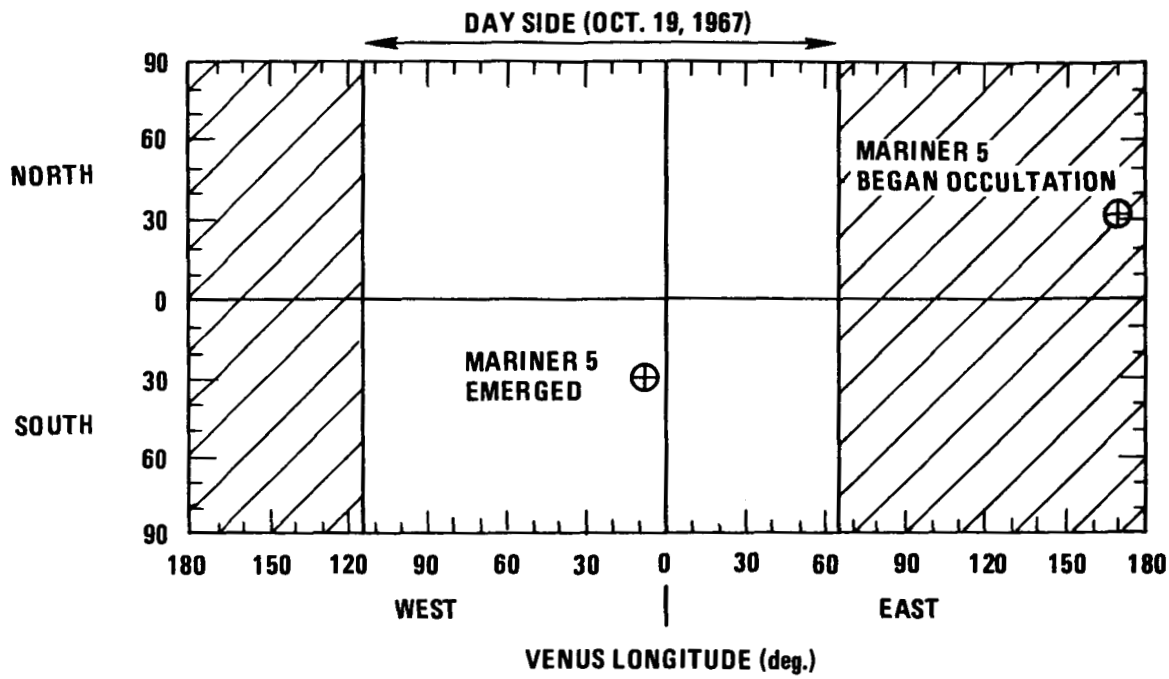

Figure 4.—Mariner 5 occultation experiment.

cated the possible presence of a plasma tail. The average interplanetary electron number density determined during the occultation was about 5.06 electrons/cm^3. Evaluation of the Lyman-alpha measurements with theoretical models of the Venus thermosphere (<9000 km) indicate that the temperature of the day-side thermosphere of Venus is about 650K (ref. 51).

Measurements were made during the occultation from about 6140 to 6085 km from the center of Venus. At the lower altitude the radius of curvature of the radio signal path became comparable to the distance to the center of mass of Venus so the signal was extinguished by severe defocusing. Data obtained from the experiments were related to the refractivity of the atmosphere, and the refractivity profiles were used to compute pressure and temperature as a function of altitude. The temperature and pressure profiles shown in figure 6 indicate little difference between the day side and the night side of Venus (ref. 49). Boundary temperatures of 150 and 250K for a 100% CO_2 atmosphere were used at an altitude of 90 km to represent extremes for computing the profiles. The fine structure in the temperature profiles between 60 and 90 km indicated a region with several relatively warm and cold layers. The average temperature lapse rate between 80 and 60 km was 4K/km. The corresponding value between 60 and 50 km was 10K/km. The change in lapse rate at about 60 km indicated the possible condensation of some vapor. Mass mixing ratios of water vapor between 10^{-3} and 10^{-2} were suggested as a possible explanation for the observed change in lapse rate.

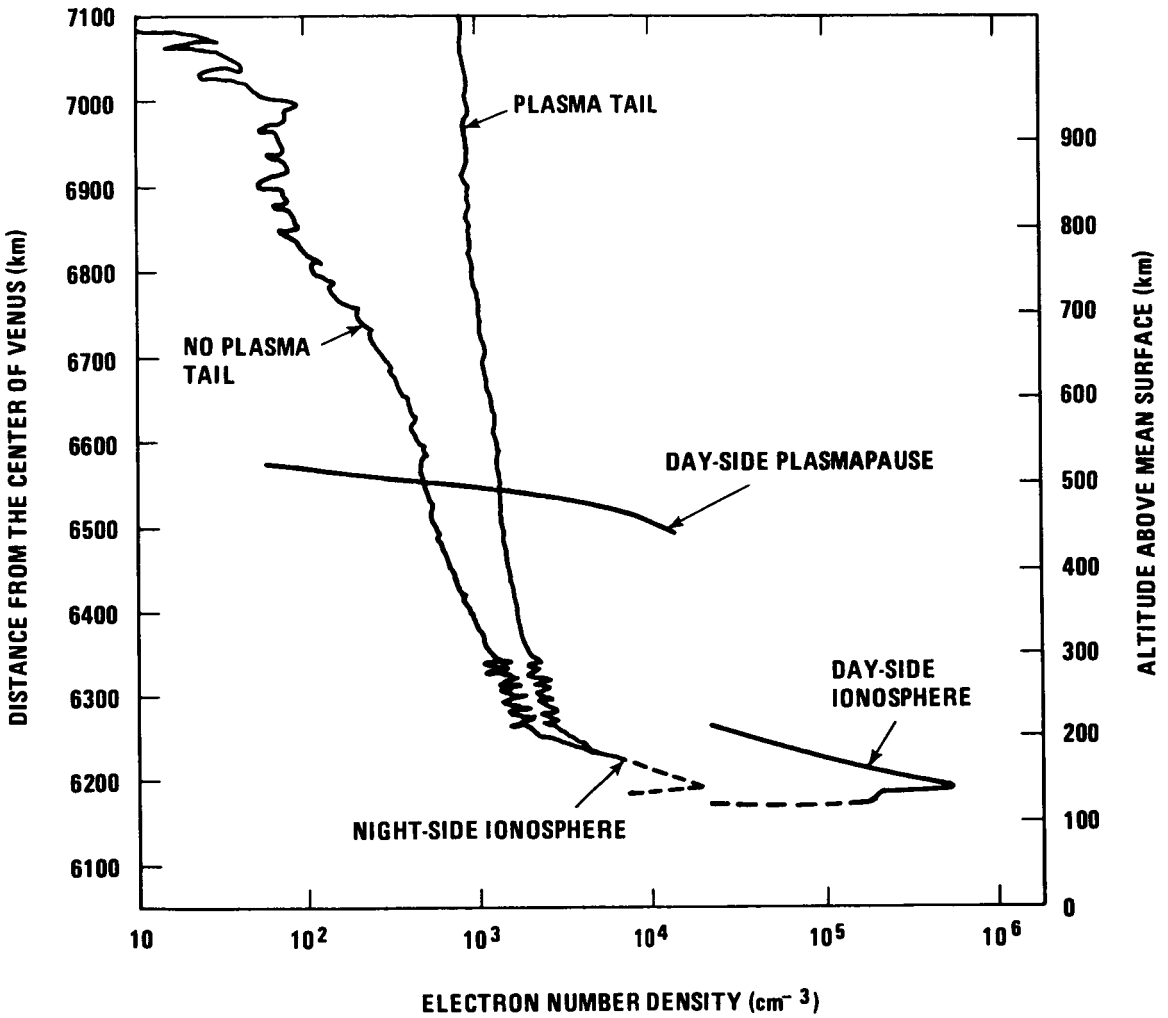

Figure 5.—Mariner 5 ionization profiles (ref. 50).

It was determined that the S-band signal suffered a propagation loss because of absorption below the 50 km. The loss profile suggested that the composition may vary with altitude (ref. 49). Accordingly, calculations were made using an atmosphere consisting of CO_2 and a microwave absorber below 50 km with the same refractivity as CO_2. The resulting profile reproduced the minimum temperature lapse rate between 50 and 45 km altitude (fig. 6). This change in lapse rate and the S-band loss profile suggested the condensation of vapor, but H_2O is an unlikely candidate in view of the high temperatures at these altitudes. Therefore, the possibility was presented for two different cloud systems, one at 60 km altitude and the other at near 50 km altitude.

2.1.2.4 Venera 5 and 6

The U.S.S.R. spacecraft Venera 5 and 6 entered the atmosphere on the night side of Venus on 16 and 17 May, 1969 at points separated by about 300 km. Venera 4 results had been

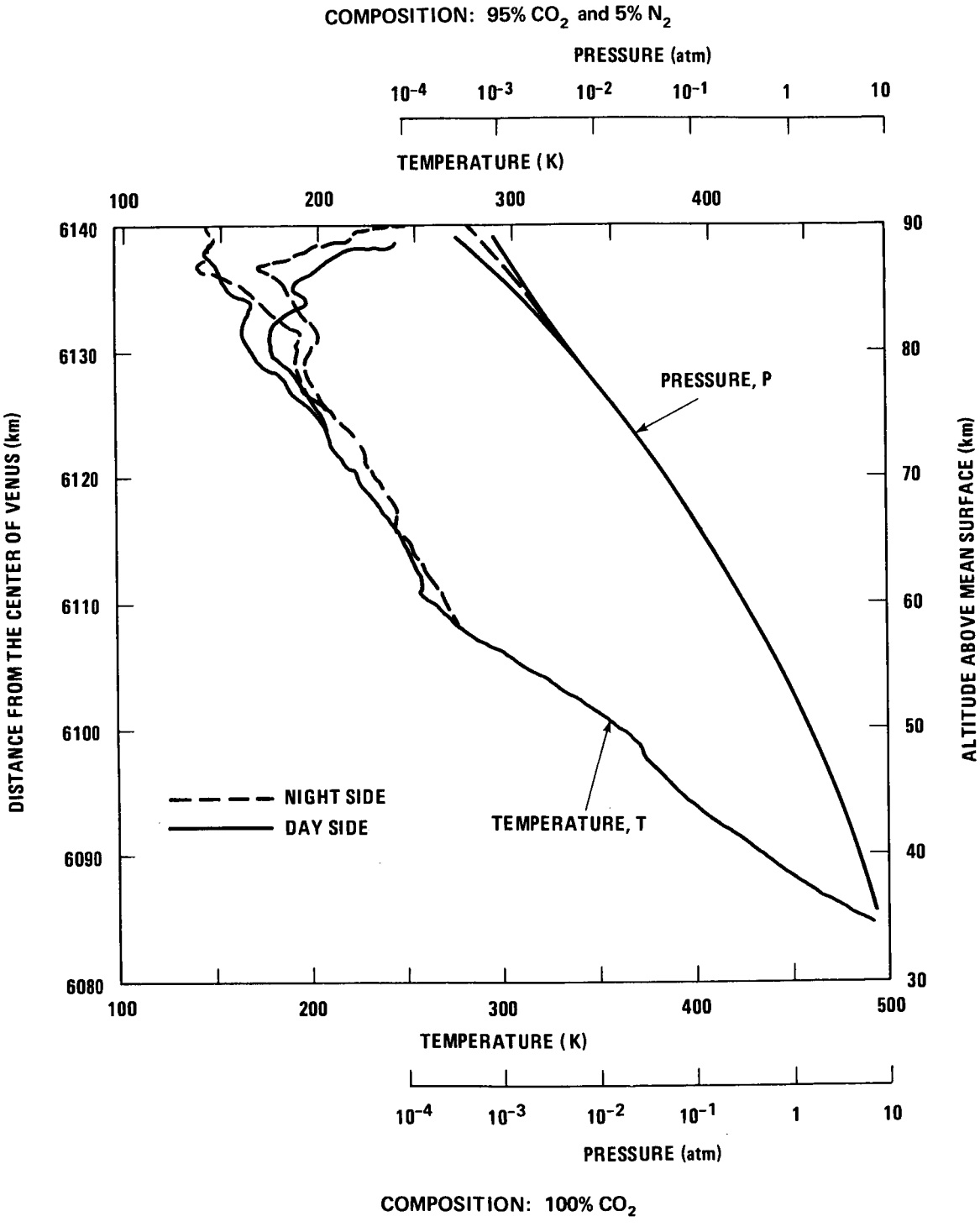

Figure 6.—Mariner 5 temperature and pressure profiles for two compositions (ref. 49).

used to improve the design of the spacecraft and the scientific equipment. Major changes in Venera 5 and 6 included a reduction of the main parachute area, an increase in the structural strength of the spacecraft, an improvement in radio altimeter operation, expansion of the range of pressure and temperature measurements, an increase in the accuracy of the gas analyzer, and installation of a different type of densitometer (ref. 39).

Distance to the surface was determined by radio altimeter which began operation after main parachute deployment and returned signals corresponding to altitude increments of 8 to 10 km. The altitude regions traversed by both spacecraft as determined by radio altimeter agreed satisfactorily with calculations made by the hydrostatic equation and the equation of state and by the equation for quasi-uniform descent of a vehicle on a parachute (ref. 40). The results of the calculations indicated that the descent velocities varied from 32 to 6 m/sec. Both radio altimeters made initial readings where the pressure was about 6.6 atm. Because the difference in length of vertical travel by Venera 5 (36.7 km) and Venera 6 (34.2 km) was within the error limits of the altimeters, the readings at the 6.6 atm level were averaged to yield an altitude 36.1 km above the surface. Data transmission ended at 20 km above the mean surface.

Both Venera 5 and 6 were equipped with gas analyzers to determine the concentrations of CO_2, inert gases, O_2, and H_2O. Measurements by Venera 5 were made at pressure levels of .6 atm and 5 atm and by Venera 6 at 2 and 10 atm. Results of the gas analysis indicated the following composition (ref. 45):

CO_2	97 (+3, – 4)%
O_2	not more than 0.1%
N_2 and other inert gases	not more than 2%
H_2O	from 6 – 11 mg/liter (at 0.6 to 2 atm pressure)

Each spacecraft was equipped with six aneroid-type manometers for pressure measurement, three resistance thermometers to measure temperature, and a tuning-fork densimeter to measure density. During each descent, 70 readings of pressure and more than 50 measurements of temperature were made beginning at the 0.6 atm level at an altitude of 56 km and ending at 20 km. The temperature, pressure, and density profiles are shown in figure 7 as a function of altitude above the mean surface. The data have been superposed so that the pressure of 6.6 atm is at 36.1 km, the average altitude. The temperature profile was near adiabatic (refs. 39 and 40). The measured density values were not consistent with the measured pressure and temperature so the density profile was calculated with the equation of state on the basis of observed temperature and pressure (refs. 38 and 39).

Analysis of the measurements indicated that the descent was smooth and that vertical currents did not exceed 0.3-0.5 m/sec (refs. 40 and 53). An indirect estimate of horizontal wind velocity was made in reference 53. Winds of 3 to 25 m/sec were estimated with the lower value more probable.

The Venera 5 and 6 water vapor measurements were used to estimate the altitude of the condensation and the thickness of the resultant clouds. The lower boundary altitude was

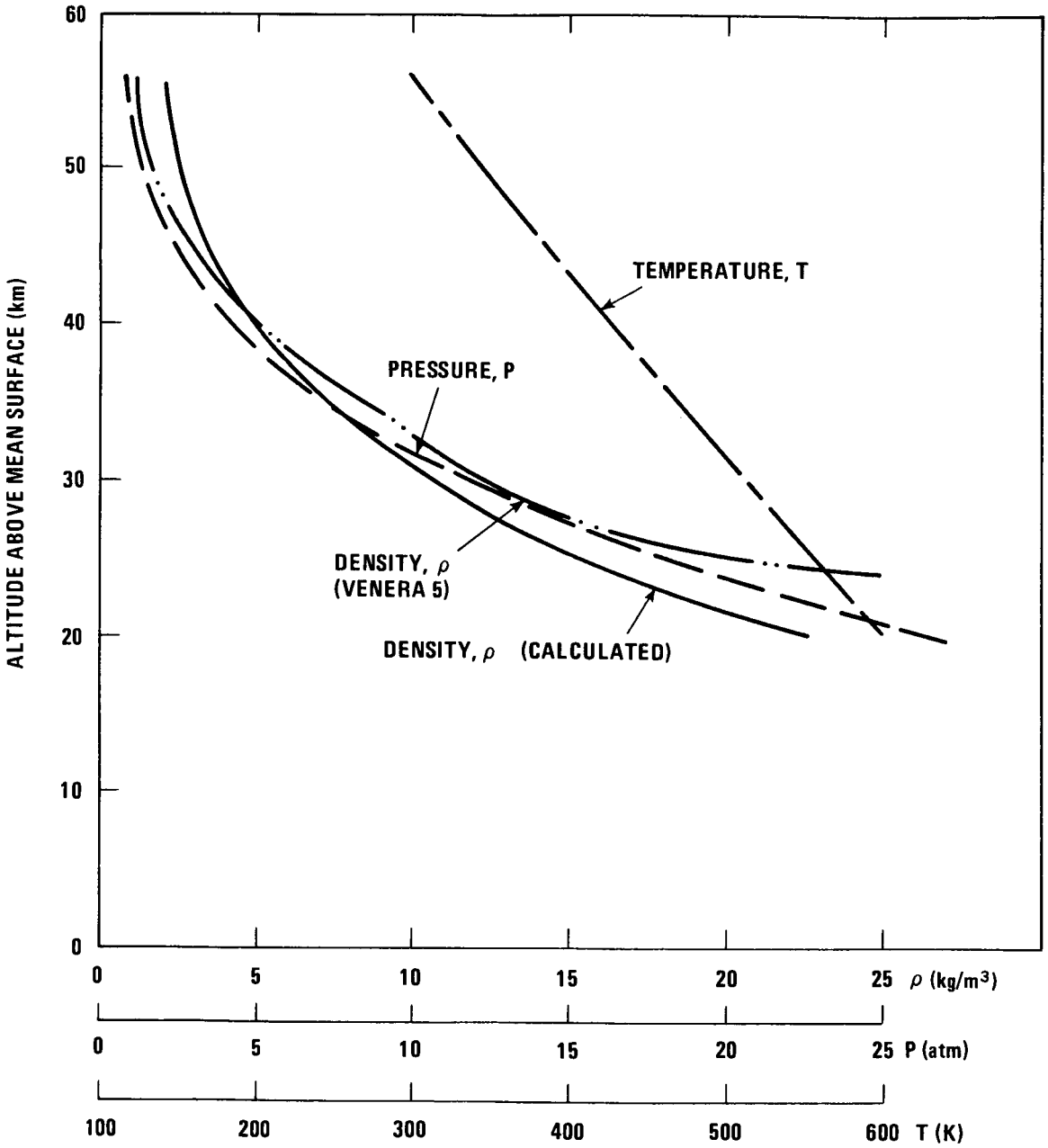

Figure 7.—Venera 5 and 6 measured data (refs. 39 and 40).

60 km and the most probable thickness of the supercooled water vapor or ice crystal clouds was 8 to 10 km (refs. 39 and 40).

Microwave attenuation was computed for the Venus atmosphere based on Venera 5 and 6 data. Radiowave absorption was calculated taking into account the measured percentages of CO_2, H_2O and O_2. It was concluded that wavelengths shorter than 5 cm should not be used for communication between Earth and the spacecraft during its landing on the surface of Venus or for operation of radio equipment in the spacecraft landing system because of the necessity of increasing the power of the transmitters and the sensitivity of the receivers (ref. 54). A related study of radiowave attenuation showed that statistical inhomogeneities of the refractive index could be an indication of turbulence in the atmosphere. Also, a singularity at 47 km in the measured data for the refractive attenuation of radio waves can be explained by the presence of an inversion layer which increases the refractive attenuation. The inversion layer could be associated with the lower boundary of a cloud layer. The singularity is weaker on the day side of Venus where the inversion would be expected to be less stable because of higher turbulence in the atmosphere (ref. 55).

2.1.2.5 Venera 7

A soft landing on the night side of Venus was made in December 1970 by the U.S.S.R. spacecraft Venera 7. Although the spacecraft had basically the same design and general structure as previous Veneras, it had been designed for a maximum of 800K external temperature and 180 atm pressure. The descent spacecraft was protected by thermal insulation and by a heat protection system. The thermal insulation maintained a favorable heat balance inside the spacecraft during its operation in the hot atmosphere and on the surface of Venus and served as a damping device during landing. The heat protection system shielded the spacecraft from the high temperatures produced by aerodynamic drag of the atmosphere (ref. 56).

Descent velocity in the Venus-Earth direction was derived from Doppler shift of onboard radio frequencies. The time history of descent velocity was used to compute height increments above the surface. Velocity measurements showed that when the descent parachute opened at an altitude of about 30 km, descent velocity decreased from 27 to 19 m/sec. At about 25 km the descent velocity unexpectedly increased from 15 to 26 m/sec, then slowly returned to the previous levels at about 10 km. The spacecraft was descending at 16.5 m/sec when it landed. Because of the recorded abrupt stop, it appeared that the surface was hard (ref. 56). Altitude was computed from the descent velocity and from the equations of an adiabatic gas on the basis of Venera 4, 5, and 6 experience. The adiabatic results indicated a descent path 2 km longer than measured by the descent velocity. The latter path deviated from the adiabatic path in the altitude region between 25 km and 5 km, which is the same region in which the descent velocity had changed abruptly.

Venera 7 was equipped with resistance thermometers and aneroid manometers to measure temperature and pressure. However, the onboard telemetry commutator remained in a fixed position and only ambient temperature information was transmitted. Measurements began at 55 km and continued to the surface where a temperature of 747±20K was measured. The

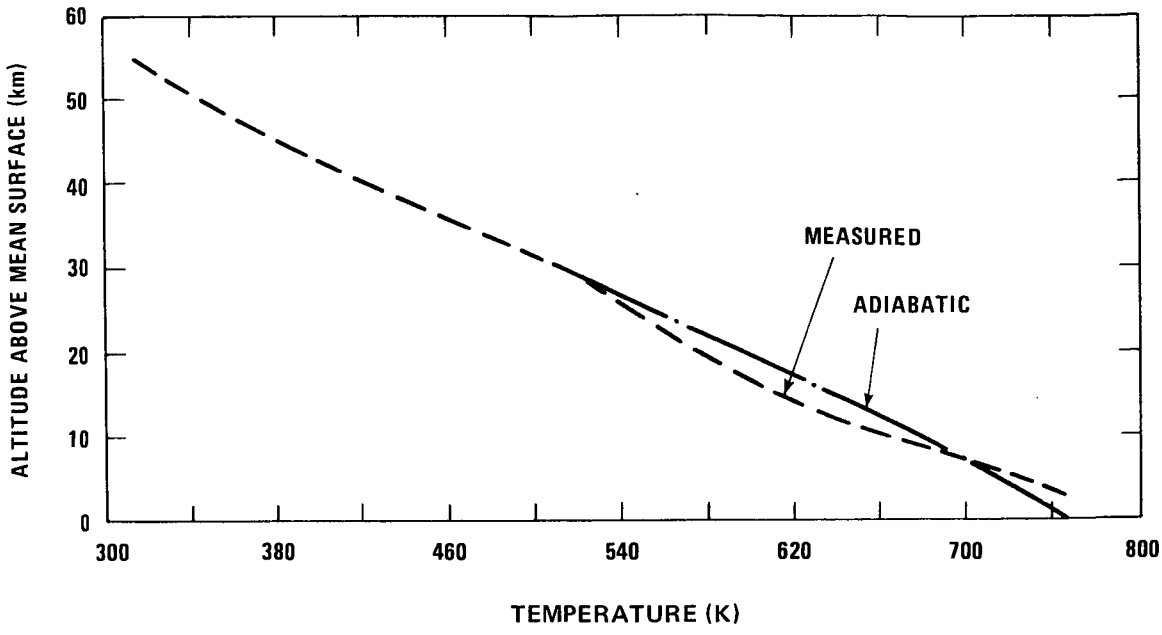

Figure 8.—Venera 7 measured data (ref. 56).

temperature profiles for the foregoing adiabatic and measured paths are shown in figure 8. The adiabatic curve was computed for a surface temperature of 747K (ref. 56).*

2.2 The Atmosphere

Discussion of the parameters applicable to the engineering models of the Venus atmosphere is divided into the lower and upper atmosphere as shown in figure 9. These regions have been subdivided into regions bearing names associated with the Earth atmosphere such as troposphere and exosphere. Planetary radius is discussed first because the value of the radius is critical to the determination of parameter values at the surface. Discussions are also included on atmospheric interaction with solar wind, clouds, and gravity.

2.2.1 Planetary Radius

Prior to the determination of the radius of Venus by radio astronomy, the only available measurements referred to the optical disc which had led to a mean value for the optical radius of 6120±8 km (sec. 2.1.1.1). Since then, however, radio astronomy techniques (table 1) have provided numerous readings of the solid planetary sphere of which the value of 6050±5 km is considered best.

*Results from the most recent U.S.S.R. spacecraft, Venera 8, became available after completion of this monograph. The conclusions and models based on the earlier data remain valid, however. Venera 8 landed and survived for 50 minutes on the surface of Venus. Preliminary reports indicated the surface pressure was about 90 atm and surface temperature about 750K. Winds of 50 m/s were detected at 45 km and winds of 2 m/s at about 10 km.

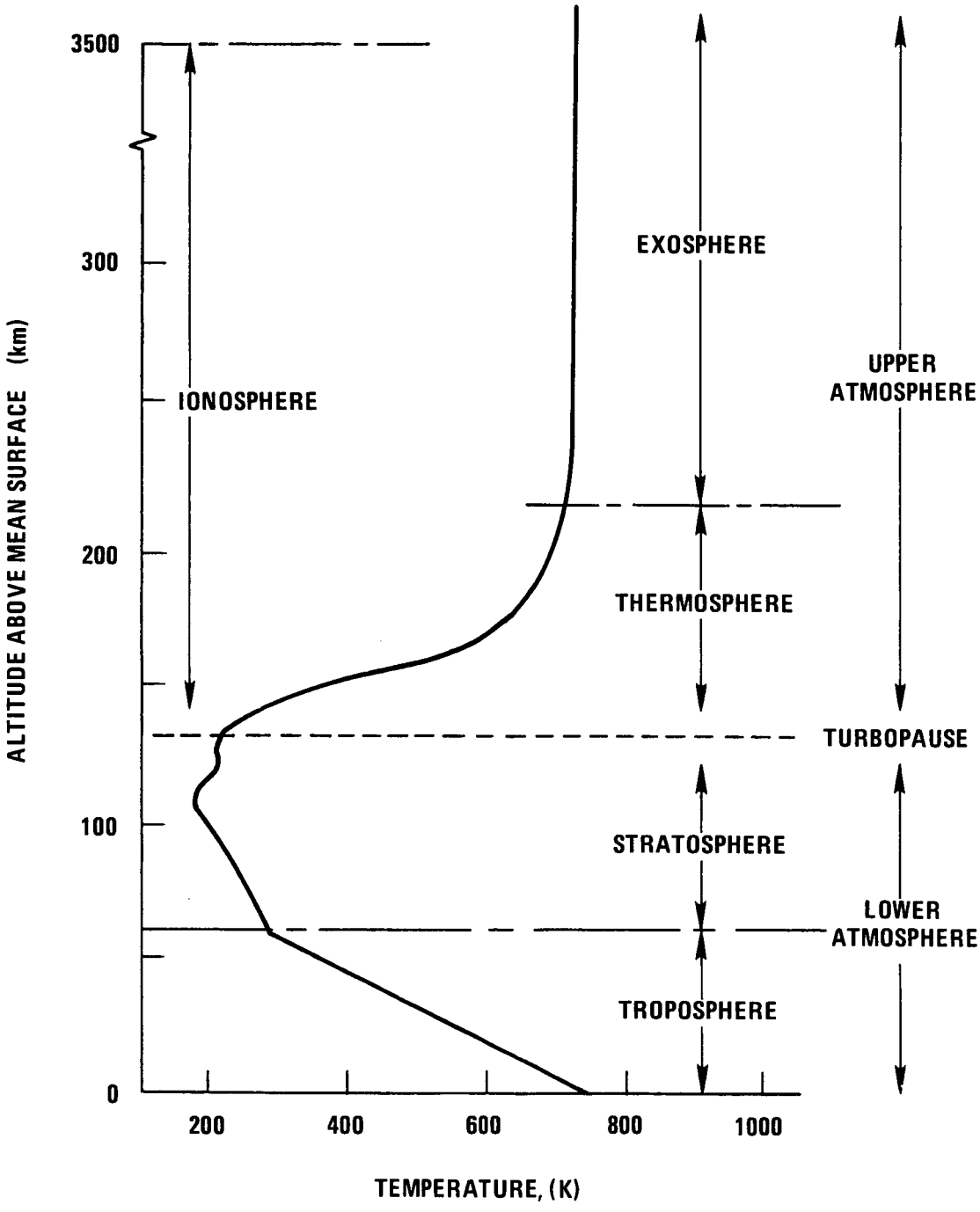

Figure 9.—Atmospheric regions of Venus.

As discussed in section 2.3.1, Venera altitude data was determined by radio altimeter readings to the planetary surface and Mariner 5 data were given as a function of Venus-centered distance, the accuracy of which depended on the Mariner 5 trajectory and the Venus orbit determinations (ref. 41). Comparison of the experimental results of Venera 5 and 6 to Mariner 5 results indicated that the mean surface level in the descent region was 6050 km (ref. 39). Mariner 5 data published in reference 49 was also referenced to 6050 km in order to determine altitude. A radius of 6050±5 km has been adopted for this monograph; the uncertainty is considered to be realistic.

Data published in reference 24 indicated surface height variations over the entire equatorial region of Venus. The highest observed elevation was a 3 km peak with a slope of about .04 degree on one side and a steep slope of .5 degree on the other side. The general area of the elevated region extended about 500 km in latitude and 6000 km in longitude.

2.2.2 Lower Atmosphere

2.2.2.1 Composition

The components of the Venus lower atmosphere have been identified by gas analysis experiments onboard the Venera 4, 5, and 6 spacecraft and by spectroscopic measurements made from Earth. Table 2 summarizes current estimates of percentages by volume of component gases in the Venus atmosphere. The major constituents are CO_2 and inert gases, principally N_2; values shown were obtained from Venera 5 and 6 measurements. The value of O_2 reflects an upper limit obtained from spectroscopic measurements. The content of oxygen as measured by Venera 5 and 6 did not exceed 0.1%, but the exact amount could not be determined because of limitations of the detector (ref. 45).

The quantity of H_2O detected by the Venera spacecraft and spectroscopic measurements are shown in table 2. The Venera values (which indicate water vapor mixing ratios of the order of 10^{-3} to 10^{-2}) are in disagreement with spectroscopic measurements which indicate water vapor mixing ratios of the order of 10^{-6} to 10^{-4} (refs. 2, 14 and 17). The spectroscopic data would appear to eliminate H_2O as the major component of the observed visual cloud at 240K. The amount of H_2O present has been widely discussed because of its importance in the theory of cloud formation, its effect on Earth-based measurements such as brightness temperature, and its effect on radiowave absorption. The Venera value is supported by several arguments. It was noted in reference 45 that the water vapor concentration decreased with a reduction in pressure. In references 3 and 36 it was indicated that the presence of a cloud layer, particularly ice clouds, could result in the moisture content above the clouds being significantly lower than that measured below the clouds. The Venera concentrations were used to show that clouds of either ice particles or supercooled water vapor could result at altitudes slightly higher than that at which Venera measurements were begun (refs. 39 and 42). The Mariner 5 results reported in reference 49 confirmed these conclusions. Comparison of theoretical studies and microwave spectrum measurements (ref. 29) also indicated a water content of 0.65±.35% in agreement with the Venera values. A similar comparison in reference 30 indicated a water vapor molar fraction of 0.4±0.3%.

TABLE 2

COMPOSITION OF THE VENUS ATMOSPHERE

Component	Estimated Per Cent by Volume	Source
CO_2	97, +3, −4	ref. 45
N_2, A, Inert Gases	< 2	ref. 45
O_2	$< 10^{-3}$	ref. 57
H_2O	$10^{-2} - 10^{-1}$ $10^{-4} - 10^{-2}$	ref. 45 ref. 2
HCl	$10^{-4.2}$	ref. 15
HF	$10^{-6.2}$	ref. 15
CH_4	$< 10^{-4}$	ref. 15
CO	$10^{-2.34}$	ref. 16
COS	$< 10^{-6} - 10^{-4}$	ref. 14
NH_3	$< 10^{-5.5}$*	ref. 14
N_2O	$< 5 \times 10^{-5}$	ref. 3
He	$\approx 10^{-2}$	ref. 3
CH_3Cl	$< 10^{-4}$	ref. 15
C_2H_2	$< 10^{-4}$	ref. 15
HCN	$< 10^{-4}$	ref. 15
O_3	$< 10^{-6}$	ref. 14
C_3O_2	$< 10^{-4.3}$	ref. 14
H_2S	$< 10^{-1.7}$	ref. 14
SO_2	$< 10^{-5.5}$	ref. 14
CH_3F	$< 10^{-4}$	ref. 15

*In contrast to the spectroscopic limit, the Venera 8 measured an NH_3 abundance between 0.01 and 0.1 percent at altitudes between 46 and 33 km.

Radiowave absorption in the presence of water vapor content between 0.1 and 0.8% was studied in reference 54. Other studies indicated that this amount of water might be sufficient to supply the infrared opacity needed to maintain the high surface temperatures of Venus (ref. 58). Studies based on thermochemical considerations suggest a water vapor content of 0.04%.

Polarization studies on the basis of refraction index, however, showed that the visual clouds could not be pure water or ice (ref. 20). In addition, numerous other cloud components such as ferrous chloride (ref. 14) were dismissed on the basis of the measured refraction index as well as chemical properties (refs. 20 and 59). Pure ice or water clouds were rejected in references 60 and 61 because liquid water present in the atmosphere would be in extremely concentrated aqueous HCl solution in the presence of the HCl that has been detected spectroscopically (table 2). Furthermore, the HCl solution would have caused the Venera gas analysers to detect the conductivity of a strong solution of a strong electrolyte and caused an erroneous reading of water content. It was argued that the mole fraction of water vapor was overestimated and should have been on the order of 10^{-4} (refs. 2 and 60). Thus, although H_2O has been identified as a constituent of the Venus atmosphere, the concentration is in question.

The Venera gas analyzers were designed to detect CO_2, inert gases, O_2, and H_2O. Other component gases listed in table 2 are derived from spectroscopic measurements except the value for the He which is an estimated amount. Other possible components derived from chemical analysis considerations are given in reference 61.

2.2.2.2 Temperature

Temperature profiles from about 90 km to the surface of Venus have been obtained by spacecraft (figs. 3, 6, 7, and 8). These profiles are compared in figure 10 with a mean planetary radius of 6050 km. The Venera 4, 5, and 6 data were adjusted to agree at a pressure of 6.6 atm and Venera 7 data was superposed at a temperature of 500K because pressure data were not recorded (ref. 56). The variation in the Venera 7 data below 27 km was discussed in section 2.1.2.5.

The data agree well in the region in which they overlap and are within rms errors. Because the Mariner 5 data were calculated from refractivity profiles which used a composition of 95% CO_2 and 5% N_2, it has been suggested that these data could be adjusted to agree more closely with the Venera data by reducing the mean molecular weight. Improved correlation has been achieved by using less CO_2, e.g., 85% (which is in conflict with the Venera composition measurements), or relatively large percentages of light inert gases, e.g., 8% He. However, there is little evidence to support these values.

The lapse rate, i.e., the change in temperature with altitude, is close to adiabatic below 50 km. The curves in figure 10 have been extrapolated to the surface with adiabatic gradients. The Venera curve was extrapolated by using the constant lapse rate that was determined from the final segment of the observed temperature data. This results in a surface temperature of 772K (ref. 40). Mariner 5 data were extrapolated by using a variable lapse

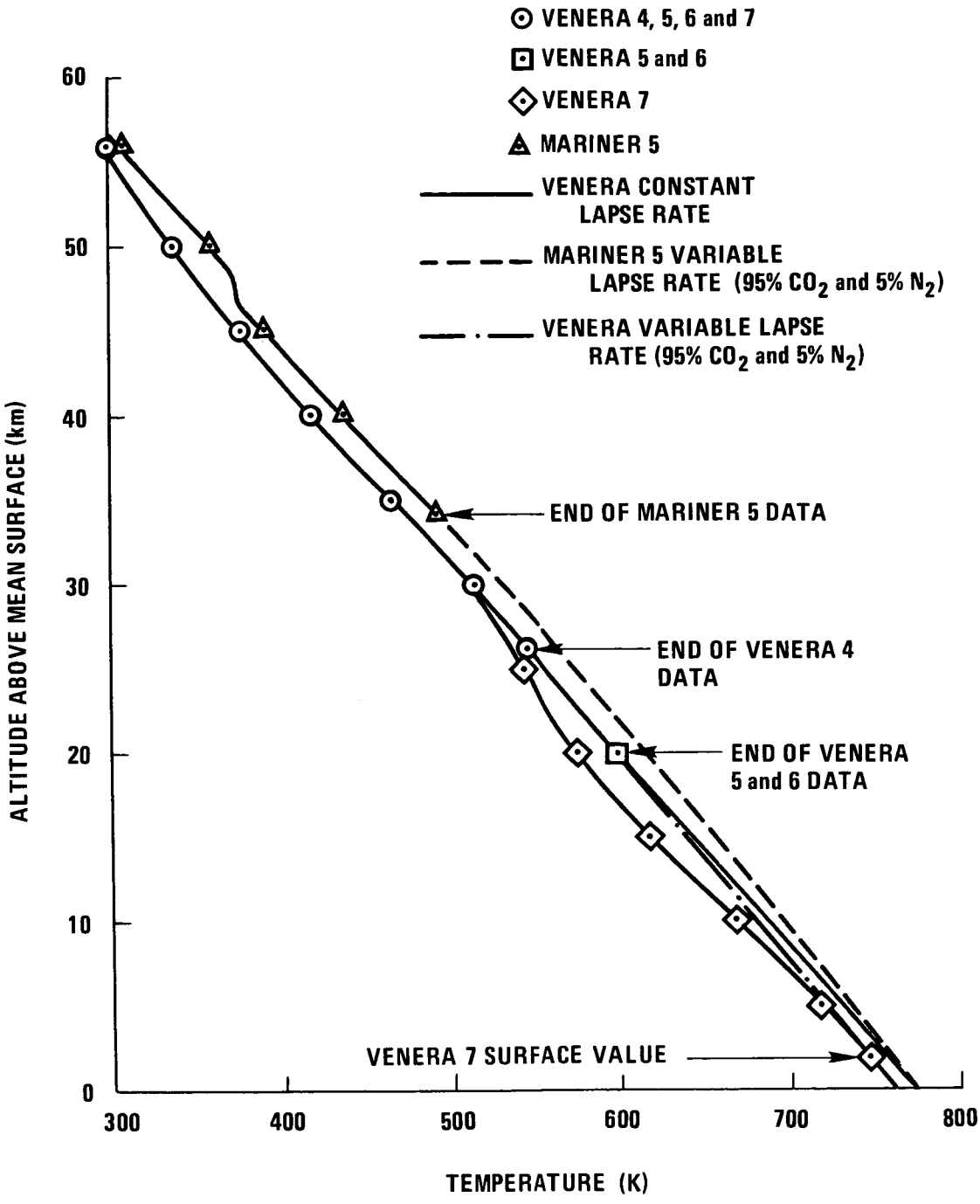

Figure 10.—Venus lower atmosphere temperature profiles.

rate for a dry adiabatic atmosphere which included effects of compressibility (ref. 62). For the calculations, lapse rates were determined for an ideal 95% CO_2 and 5% N_2 atmosphere. Changes in compressibility and molecular weight had little effect on the extrapolated value of surface temperature, 774K. Extrapolation of the Venera data by the same method yielded 761K at the surface. At 2 km above the mean surface, a temperature of 746K was computed which corresponds to the surface value observed by Venera 7. A possible discrepancy of 2 km in measured altitude for Venera 7 is noted in section 2.1.2.5.

Extrapolations of Venera data were also made which assumed that the temperature gradient tends toward an isothermal condition at the surface (refs. 40 and 63). A surface temperature of about 720K was predicted for a 5 to 10 km isothermal layer. A parameter study was conducted on an adiabatic model with an isothermal layer at the surface in order to verify brightness temperature measurements of 700±50K at 6 cm (ref. 29). Results indicated that the surface temperature should be 770±25K and the isothermal layer less than 4 km in order for the model to predict the observed brightness temperature.

Large-scale differences in the surface temperature across the planetary disc have not been observed (sec. 2.1.1). Also, the Mariner 5 occultation experiment indicated only minor diurnal temperature changes in the lower atmosphere, as shown in figure 6.

The temperature profile between 60 and 90 km obtained from Mariner 5 (fig. 6) was correlated with results derived from Earth-based measurements at altitudes where cloud layers are believed to exist. Emissions in the near-infrared wavelengths measured by Mariner 2 were interpreted to give a temperature at the top of the clouds of 240K (sec. 2.1.2.1). These values agreed with similar Earth-based measurements which yielded temperatures between 215 and 250K (ref. 2 and 21). In addition, spectroscopic studies have defined the effective cloud top temperature between 220 and 280K (ref. 2). The marked change in lapse rate at about 60 km in the Mariner 5 data (figure 6) has been interpreted to indicate the presence of a cloud layer. The Mariner 5 temperature of 260K at this altitude also supports this interpretation (ref. 17). The presence of a cloud layer at about 60 km was also inferred from Venera investigations (secs. 2.1.2.2 and 2.1.2.4).

The upper cloud or haze layer has been identified by ultraviolet photographs (ref. 14) and by observations made as Venus transits the Sun. Measurements taken during the more recent observations indicate that the temperature at this cloud level is 180K which corresponds well with the temperature minimum of the Mariner 5 data at about 81 km (ref. 17).

2.2.2.3 Surface Pressure

Direct measurements of atmospheric pressure on Venus were obtained by Venera 4, 5, and 6 (figs. 3 and 7) and during the Mariner 5 occultation experiment (fig. 6). The pressure profiles are compared in figure 11 for a mean planetary radius of 6050 km. The Venera 4, 5, and 6 data were adjusted to agree at a pressure of 6.6 atm (ref. 39). The Venera and Mariner 5 profiles agree remarkably well.

Because surface pressure was not measured, the profiles of figure 11 have been extrapolated to the surface with the adiabatic gradients used for the temperature extrapolation (sec.

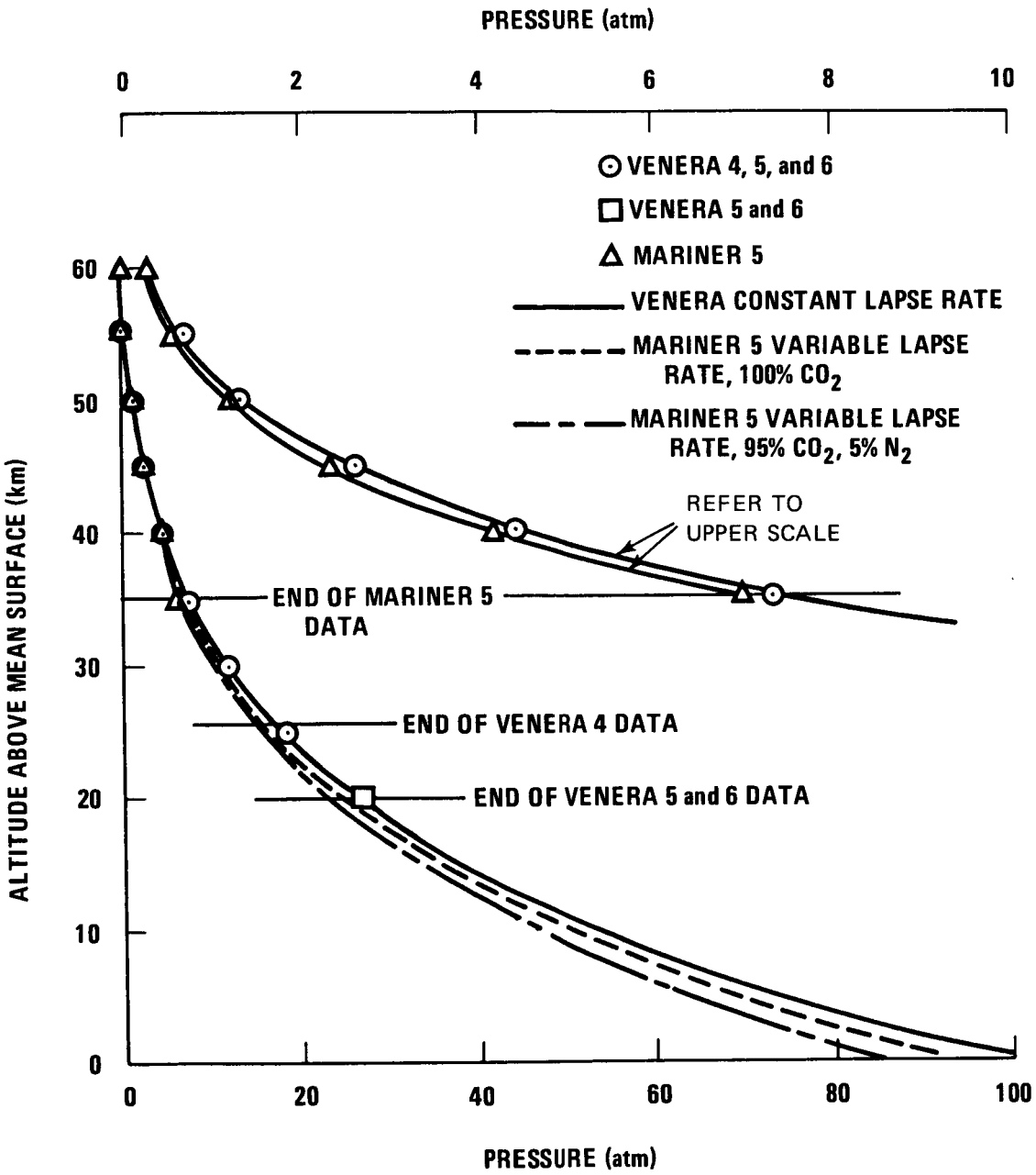

Figure 11.—Venus lower atmosphere pressure profiles.

2.2.2.2). Extrapolation of the Venera data with a constant lapse rate results in a surface pressure of 102 atm (ref. 40). With a variable lapse rate (ref. 62), a surface pressure of 94 atm was determined from Mariner 5 data for an atmospheric composition of 100% CO_2 and 86 atm for a composition of 95% CO_2 and 5% N_2. Extrapolation was begun at 35 km, the lowest value of pressure determined from the Mariner 5 data. A similar extrapolation of Venera data at 20 km results in a surface pressure of 100 atm for a 95% CO_2 and 5% N_2 atmosphere.

Pressure profiles for Venera 7 were computed from the temperature profiles with the hydrostatic law and the equation of state. Surface values for the adiabatic and measured paths (section 2.1.2.5) were 86 and 97 atm (ref. 56). Surface pressure determined from Venera data with an assumed isothermal condition near the surface resulted in a predicted pressure of 107 atm (ref. 40). A value of 95±20 atm has been deduced from a model used to correlate radio brightness measurements (ref. 29).

The resolution of an appropriate uncertainty range for the mean surface pressure is a direct consequence of the planetary mean surface radius. As noted in reference 2, surface pressure lies in the range of 70 to 120 atm which is considerably better than the 3 to 1000 atm range which existed prior to the accumulation of the spacecraft data (ref. 64).

2.2.2.4 Density

Density values measured by Venera 4, 5, and 6 (figs. 3 and 7) were not consistent with measured pressures and temperatures so a density profile was calculated (sec. 2.1.2.4). Surface density values were 67 kg/m^3 for adiabatic and 78 kg/m^3 for isothermal extrapolation (ref. 40).

Number density was calculated from refractivity data obtained during the Mariner 5 occultation experiment for planetocentric distances between about 6085 and 6140 km. These data are compared to calculated values in figure 12 (refs. 65 and 66). The Regulus occultation density value at 6169 km (ref. 43) is also given in figure 12.

2.2.2.5 Winds

The nature and theory of the general circulation of Venus' atmosphere remain uncertain although considerable progress has been reported in recent years (ref. 67). The only observational data relevant to the question of atmospheric winds refer to regions of the atmosphere above the visible clouds. The wind field at greater depths must be inferred on the basis of detailed theoretical models.

Pictures of Venus taken in ultraviolet revealed a variety of features (ref. 68). Ultraviolet markings traveled around the planet with an apparent period of 3.6 to 4.5 days. A rotation period of this magnitude implies zonal velocities of the order of 100 m/s, some 50 times larger than the rotation speed of the solid planet at the equator. More recent photographic data, reviewed in references 69 and 70, confirm the earlier work and strongly imply retrograde rotation of the Venus atmosphere with a period of 4 to 5 days in the vicinity of

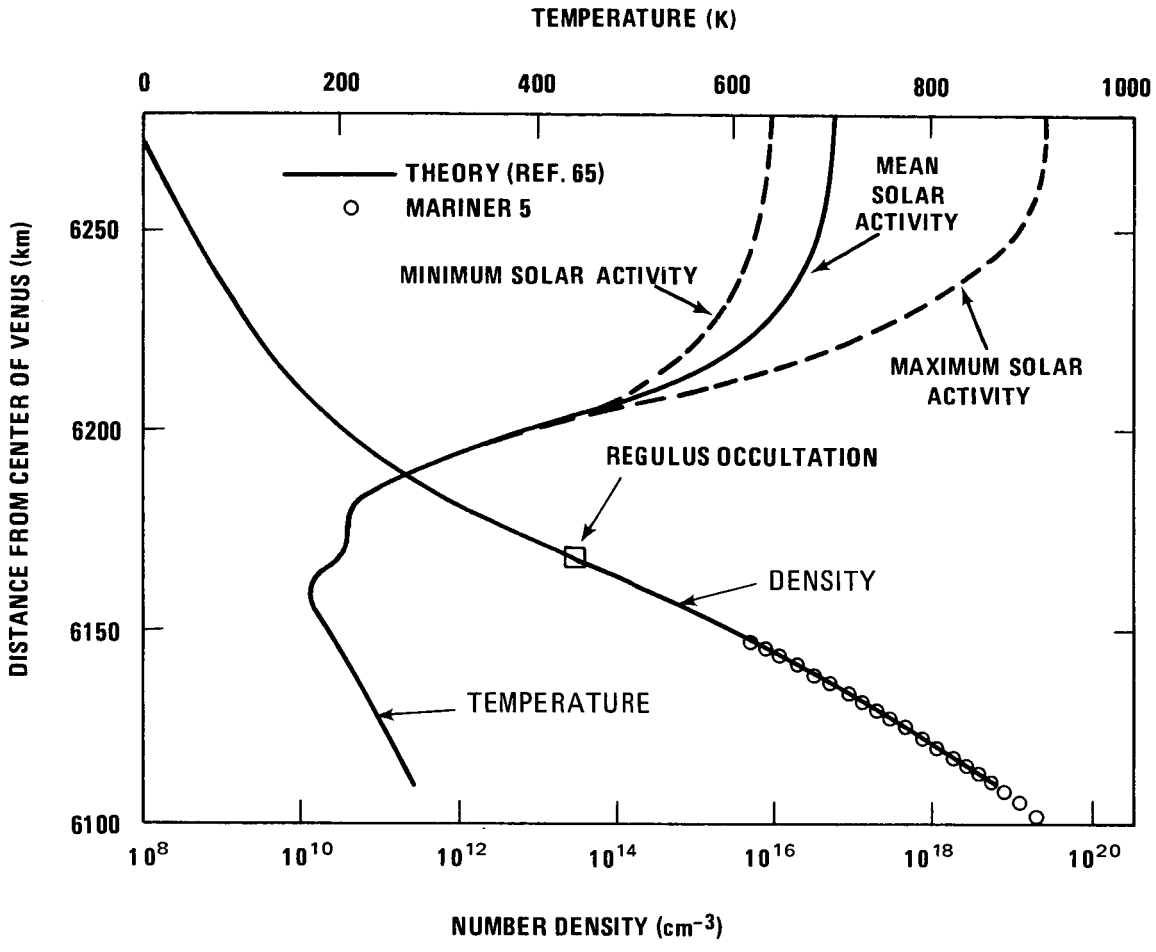

Figure 12.—Model of Venus neutral atmosphere and measured density data (refs. 65 and 66).

the ultraviolet clouds. Independent support for this surprising result is provided by recent spectroscopic observations (refs. 71 and 72) in which significant Doppler shifts were detected in the solar spectrum reflected by Venus. These shifts were interpreted to indicate retrograde velocities of about 100 m/sec, equivalent to an estimated rotation period of 4.3±0.4 days.

The observed zonal wind speeds are unexpectedly large, comparable with zonal circulations in the Earth's atmosphere at high latitudes. High zonal wind speeds can be understood for the Earth in terms of the differential angular momentum available on a planet with a rapid rotation period, 24 hours. Evidently a different mechanism is operative for Venus; a variety of possible models are discussed in references 70, 73, and 74. There is general agreement that zonal winds on Venus result from the apparent motion of the Sun during the Venus solar day. The relative motion of the heat source (Sun) and Venus sets up a typical convection cell. The convection cell is tilted because of the finite time required for diffusion of heat. Consequently, the cell develops an average Reynolds stress which acts to maintain a steady zonal flow. The magnitude of the flow is limited by the mean viscous stress.

Strong support for the moving heat source mechanism is provided by laboratory experiments with mercury, a fluid characterized by an extremely low Prandtl number (ref. 75). In these experiments a moving flame was applied to an annulus; the result was a steady rotation of the liquid in a sense opposite to the motion of the flame. The magnitude of the observed flow velocity was approximately four times larger than the velocity associated with the flame. Various theoretical discussions confirm the applicability of the moving flame model to Venus and yield velocities which are typically in the order of 100 m/sec. Although details of the models remain obscure, there are reasons to believe that an atmospheric probe entering the Venus atmosphere will encounter significant zonal winds (~100 m/sec) at least above the visible cloud deck.

The first comprehensive attempt to model atmospheric dynamics below the cloud deck was reported in reference 76 and extended in reference 77. A two dimensional Boussinesq model was used for the atmosphere which assumed that heat was applied and removed at the upper boundary (visible clouds) and that the Rossby number was small so that effects of rotation would be minor. A computer simulation of the circulation of the atmosphere was based on models similar to those of reference 76 (ref. 78). Results indicated that the day-side mean temperature is several tens of degrees higher than that of the night side and that the typical wind speed is close to 5 m/s.

Numerical models (one a Boussinesq model and another in which basic stratification of density was considered) were used to investigate circulation deep in the atmosphere (ref. 79). Two extreme cases were considered. First, rotation was neglected and the subsolar point was fixed. Second, solar heating was averaged over a Venus solar day and rotation was included. In order to account for the observed temperature profile in the deep atmosphere, it was necessary to assume significant penetration of sunlight to the near surface region, as much as 6% at the equator. The horizontal velocities are generally small below 30 km, less than 1 m/sec, but may be significant at higher altitudes. The models yield meridional velocities as large as 30 m/sec near 50 km. A typical pattern is shown in figure 13. Vertical velocities are generally small except for a narrow region of descending air near the poles, at latitudes of about 75° to 85°. Here, vertical velocities may approach 1 m/sec. Elsewhere, vertical velocities are expected to be of order of or less than 1 cm/sec.

Atmospheric winds determined for Venera 4, 5, and 6 correlate well with the theoretical winds. Vertical velocities of 1.0 to 1.5 m/sec were obtained from Venera 4 and 0.3 to 0.5 m/sec for Venera 5 and 6. Estimated horizontal winds of 3 to 25 m/sec for Venera 5 and 6 were of the same order of magnitude as the winds measured during the last 18 to 20 km (<50 km altitude) of the descent of Venera 4 (ref. 53).

2.2.3 Upper Atmosphere

The only measurements which pertain directly to conditions in the upper atmosphere of Venus are the electron density profiles obtained from Mariner 5 and the ultraviolet airglow data obtained from Mariner 5 and Venera 4. Therefore, engineering models for the upper atmosphere must rely on a variety of theoretical studies. The range in the models, however, has been limited by spacecraft results.

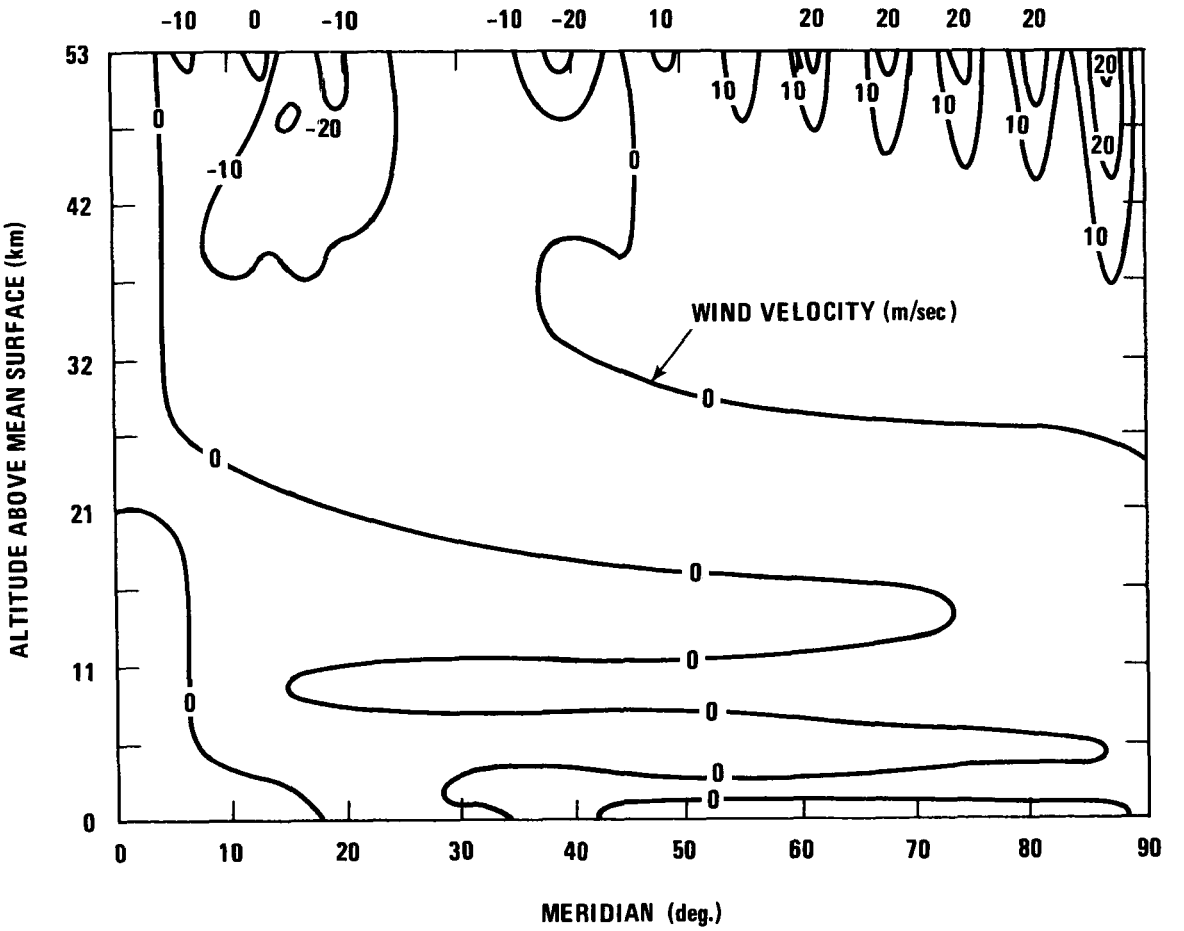

Figure 13.—Typical horizontal wind patterns (ref. 79)

2.2.3.1 Ionosphere

Mariner 5 observed an extensive ionosphere on both day and night sides of Venus (ref. 50). Occultation on the day side occurred at a solar zenith angle of 33°. The peak value for electron density was about $5 \times 10^5/cm^3$ at a planetocentric distance of 6190 km. The electron density, as indicated in figure 5, remained high ($>10^4/cm^3$) to an approximate planetocentric distance of 6500 km. At greater distances, the electron density decreased rapidly to typical values for the undisturbed interplanetary medium. The peak value for electron density on the night side was about $2 \times 10^4/cm^3$, and the night-side ionosphere was surprisingly extensive. Significant electron density ($>10^2/cm^3$) was observed to a planetocentric distance of at least 6800 km. Some evidence exists that on the night side a plasma tail extends to planetocentric distances of at least 7200 km. The ionosphere at high altitudes is believed to be controlled in large measure by electromagnetic interactions with the solar wind.

Mariner 5 carried ultraviolet photometers sensitive to radiations emitted by atomic hydrogen and atomic oxygen (ref. 80). The resulting measurements provide data for the day and

night sides of the planet. Venera 4 carried similar instrumentation, but the planetary data are limited to conditions during probe descent on the dark side of the planet (ref. 81). Neither experiment showed any evidence of significant abundances of atomic oxygen; both experiments revealed an extensive hydrogen corona. The Mariner results indicate a day-side exospheric temperature of about 650K (refs. 52 and 82), which is consistent with the plasma scale heights observed in the S-band occultation experiment. Other interpretations of the Mariner data suggested appreciable abundances of H_2 and deuterium in the upper atmosphere (refs. 83, 84, and 85). The evidence is considered weak, however, so models requiring large concentrations of these elements are viewed as highly speculative.

Models of the ionosphere already in the literature assume that CO_2^+ is the dominant positive ion (ref. 66). Increased understanding of Mars, however, has led to the expectation that O_2^+ is probably the important component. It is produced by reaction of CO_2^+ with O.

2.2.3.2 Neutral Atmosphere

The major uncertainties in neutral densities of the upper atmosphere relate to the location of the turbopause and the abundance of light constituents, O, N_2, CO, and He at the turbopause. The relative abundance of these gases is expected to increase rapidly with increasing altitude. The drag experienced by an orbiting spacecraft will be particularly sensitive to O and He, but knowledge concerning abundances of these constituents is minimal.

Atomic oxygen is produced copiously by photodissociation of CO_2. On theoretical grounds one might expect atomic oxygen to be a dominant species in the upper atmosphere. However, detailed theoretical analysis of the ionospheric profiles suggests that oxygen is a minor constituent ($<10\%$) at the ionospheric peak, as is the case for Mars; Venus models are constructed subject to this constraint.

There is no positive evidence for helium, but it has been noted that apparent discrepancies between Mariner 5 and Venera data in the lower atmosphere may be removed if Venus' atmosphere includes a significant abundance of He ($\sim 5\%$). Moreover, the extended nighttime ionosphere can be understood if helium is a major component of the upper atmosphere (refs. 85 and 86). Although the evidence is inconclusive, engineering models must allow at least for the possibility of a significant helium concentration. The lifetime of an orbiting spacecraft is affected by the assumed value for the mixing ratio of He at the turbopause.

The neutral atmosphere of Venus is described by the theoretical thermal model shown in figure 12 (refs. 65 and 66). The model yielded an exospheric temperature of 700K. This value compares favorably with the value of 650K derived in reference 82 from Mariner 5 Lyman-alpha results. The model has also been applied to the ionosphere (ref. 66).

The exospheric temperature varies with solar flux. Estimates for Venus exospheric temperatures at periods of minimum and maximum solar activity are shown in figure 12. Table 3

TABLE 3

VARIATION OF UV FLUX* AND EXOSPHERIC TEMPERATURE WITH SOLAR ACTIVITY

Solar Activity	Ratio of UV Flux to Solar Min UV Flux	Exospheric Temperature (K)
Minimum	1.0	625 ± 200
Mean	1.5	710 ± 200
Maximum	3.0	931 ± 300

*Below 1000 Å wavelength.

shows estimates for the variation of solar ultraviolet (UV) flux below 1,000 Å and the estimated exospheric temperatures for minimum, mean and maximum solar activity. The values for mean solar activity are for the time of the Mariner 5 Venus flyby on October 19, 1967.

2.2.3.3 Dynamics

Preliminary models for dynamics of the upper atmosphere suggest that the night side may be significantly colder than the day side (ref. 87). The night-side exospheric temperature could be as low as 250K, compared to day-side values of about 750K. If valid, the dynamic studies imply large lateral gradients in the neutral density from day to night. Lifetimes for orbital spacecraft would then depend critically on the position of the perigee because orbits with perigees on the dark side of the planet would encounter markedly less drag than orbits with perigees at similar heights on the sunlit side. To take into account the possibility of a low night-side exospheric temperature, an appropriate model has been developed for this monograph.

2.2.4 Interaction with Solar Wind

Analysis of Mariner 2 magnetometer measurements showed that the magnetic field of Venus is negligible (ref. 10). Thus, the planet apparently is not shielded by a magnetosphere, as is the Earth so the solar wind can interact directly with the Venus upper atmosphere. A similar situation is found for Mars where a standing bow shock wave is believed to form as the solar

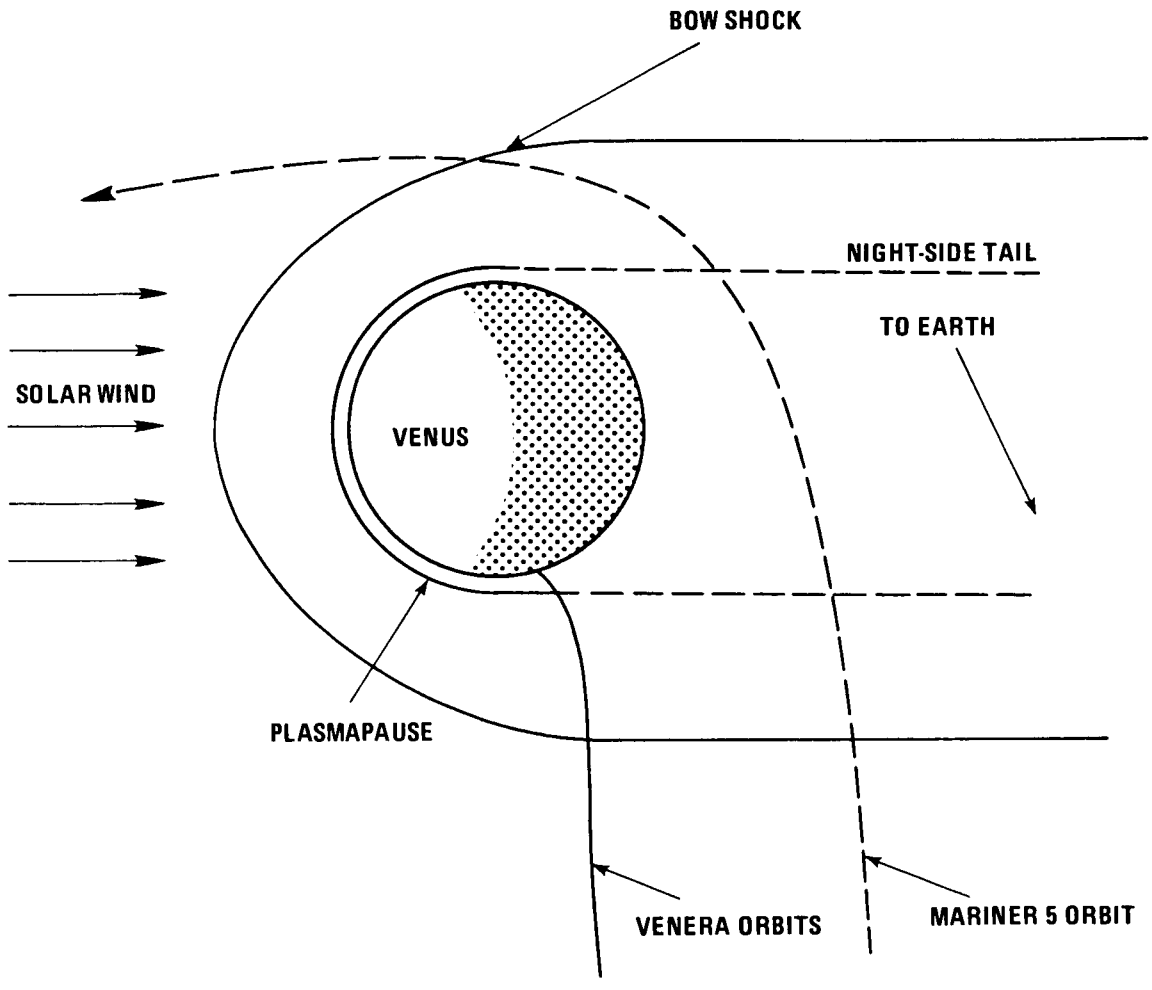

Figure 14.—Bow shock formation for Venus (ref. 85).

wind impinges on the atmosphere with resulting sharp density gradients between the solar wind and the upper atmosphere (ref. 88).

Such gradients were observed for Venus. The day-side electron density detected during the Mariner 5 occultation experiment terminated at an altitude of about 500 km (fig. 5). This termination point, called the plasmapause (or ionopause), has been attributed to the presence of a bow shock as shown in figure 14 and has been the subject of several papers (refs. 85, 89, 90, and 91).

The most prevalent theory of the shock wave formation is based on reference 88 which postulates that the magnetic field of the solar wind is compressed against the ionospheric plasma. This compression results in the formation of electromagnetic forces which deflect the solar wind around Venus. The pressure of the solar wind is balanced by the pressure of the ionosphere and the pressure of the compressed magnetic field. The plasmapause is identified as the sharp gradient between the uncompressed solar wind magnetic field and the compressed magnetic field which prevents intermixing of the solar wind and the ionospheric plasma.

In reference 90, it is proposed that a magnetohydrodynamic shock wave is formed as the magnetized supersonic plasma flow (solar wind) interacts with the planetary ionosphere. Most of the subsonic flow on the planetary side of the shock wave is deflected around Venus. Between the ionosphere and shock wave, the dynamics of the interaction of the solar wind and ionosphere indicates that the plasma is compressed more than the magnetic field. The result is a region called the plasmapause where there is a balance of pressure between the plasma and the solar wind.

The presence of a bow shock wave has not been firmly established. Reference 92 noted that Venus probe data does not include a sharp shock; in fact, flow density changed over a distance comparable to the radius of Venus. This suggests that the interaction may be similar to that between the outer regions of a comet and the solar wind which does not form a shock wave.

2.2.5 Clouds

Knowledge of clouds is important for spacecraft design and the design and operation of instrumentation for observing the Venus atmosphere. Possible adverse effects include absorption or distortion of radio transmissions and microwave observations, distortion of optical observations, corrosive action by aerosol or other cloud particles, and undesirable chemical action. The existence of two cloud layers in the Venus atmosphere was revealed by photographs taken in infrared and ultraviolet wavelengths (sec. 2.1.1.1). The upper layer is opaque to ultraviolet but transparent to infrared, whereas the lower layer is opaque to both ultraviolet and infrared wavelengths.

Information on the clouds has been obtained from radio brightness measurements, polarization studies, spectroscopic and interferometer observations, and spacecraft experiments. The

data generally agree that at least two cloud layers exist and that the temperature of the lower layer is approximately 240K and at a level of about 60 km above the mean surface. However, there is disagreement about cloud composition and the nature of the upper clouds.

The composition, particularly the presence of water vapor, and temperature of the clouds have been discussed in sections 2.2.2.1 and 2.2.3.1. Data concerning the clouds indicates that (ref. 17)

1) the top of the upper layer is at an altitude of 81 km with a pressure of .003 atm and temperature of 175K, and

2) the top of the lower layer is at an altitude of 61 km with a pressure of .240 atm and temperature of 260K.

Because the opacity of the atmosphere cannot be explained on the basis of pure CO_2, other constituents have been proposed. Dust has been suggested as a principal component of the clouds, but results of radio brightness studies (ref. 29) and polarization observations (ref. 20) indicate that dust cannot be a major component of the visible cloud decks. Other components such as H_2O, C_3O_2, $FeCl_2$ and NH_4 Cl (fig. 1) have been proposed with little supporting evidence refs. 17 and 60).

The presence and importance of water vapor in cloud formation is still open to question (sec. 2.2.2.1). Water vapor may exist in the form of HCl solutions (refs. 60, 61 and 93 and an HCl-H_2O system is presently the leading contender as the major constituent of the upper cloud layer.

The level and temperature of the lower cloud level have been established, but its composition is open to question. As noted in section 2.2.2.1, water in the amounts detected by the Venera spacecraft can be used to explain the clouds at about 60 km. These explanations are supported by Mariner 5 temperature measurements (ref. 49). However, analysis of the geochemistry of Venus (ref. 60) suggests mercury compounds (specifically, a thin haze of Hg_2Cl_2 overlaying a deep cloud of mercury droplets) as more likely components of the lower cloud layer (fig. 15). If these compounds are the main cloud constituent, they could cause the observed pale yellow tint of Venus observed from Earth. Mercury compounds could complicate radio-wavelength studies of the phase effect and meridional temperature gradients.

Possible cloud layers have been identified from Mariner 5 occultation data at temperatures of 402K (corresponding to an altitude of 44 km) and of 371K (corresponding to an altitude of 47 km) (ref. 94). Reference 60 proposes a chemical model of the atmosphere with mercurious bromide (HG_2Br_2) at 44 km and mercurious iodide (HG_2I_2) at 47 km (fig. 15). Cloud layers in the 37 to 50 km region were postulated on the basis of the S-band loss coefficient observed by Mariner 5 (sec. 2.1.2.3). Also studies of the refractive index in reference 55 indicated the possible presence of an inversion layer on the night side of Venus at an altitude of 47 km which could be associated with the lower edge of a cloud layer.

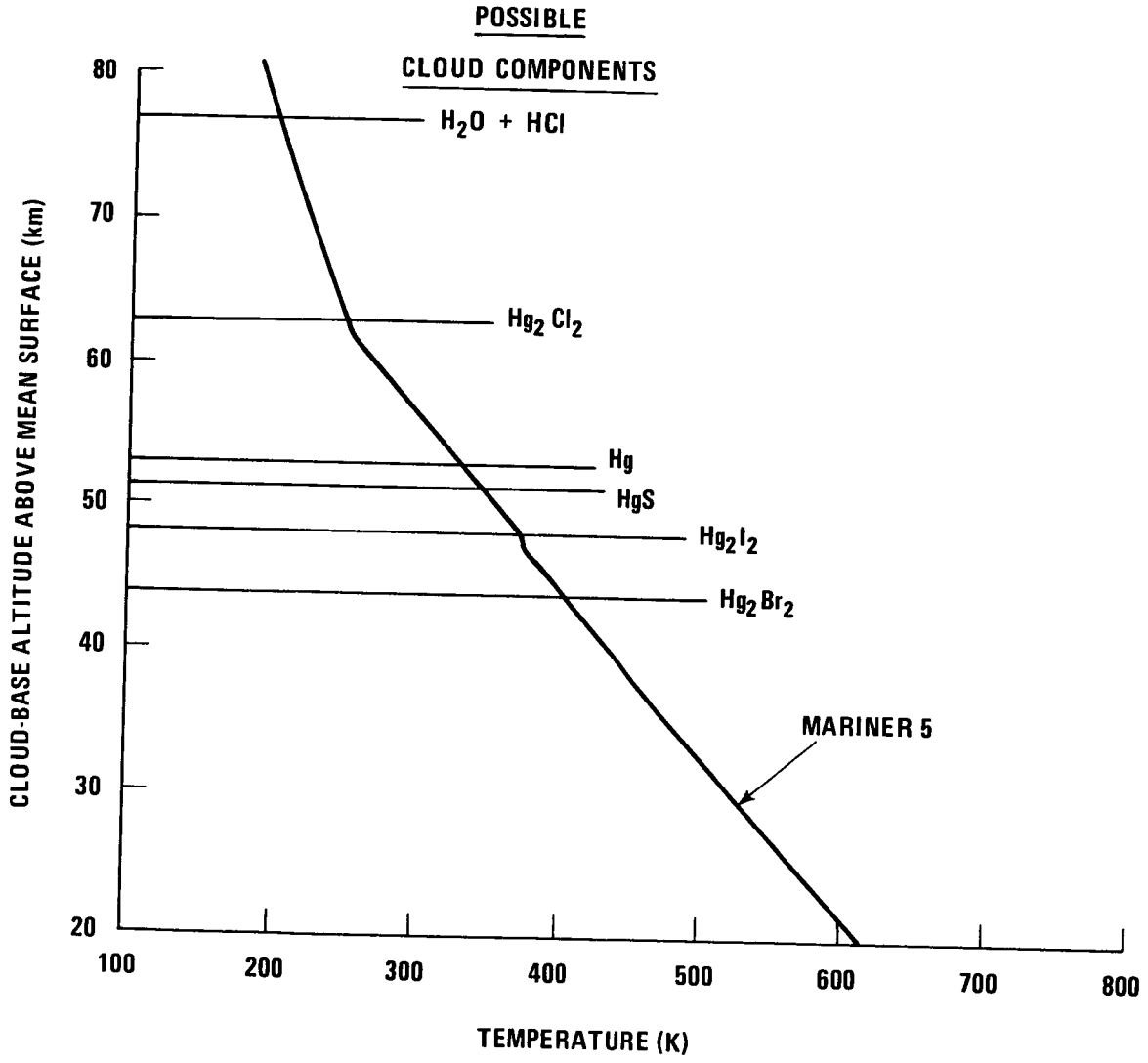

Figure 15.—Cloud layers and proposed components on Venus (ref. 60).

2.2.6 Gravity

The acceleration of gravity g_o at the surface of Venus* with a radius of 6050 km is derived from the Venus gravitational constant of $GM_{\varphi} = 324{,}873.5\ km^3/s^2$ measured by Mariner 5 (ref. 95).

2.3 Atmospheric Models

2.3.1 Calculation

The models presented in this monograph were generated by the computer program described in reference 96. The program was modified to include a molecular mass subroutine (based on the molecular mass variation with altitude), an extended temperature range for the calculation of the specific heat and the reduced collision integral which appears in the viscosity relationship, an extended pressure range for the calculation of the specific heat (based on the data of references 97 and 98), and thermochemical data which allow for the inclusion of atomic oxygen as a component gas.

The basic inputs to the computer program are the temperature profile, the surface pressure, the near-surface atmospheric composition and corresponding molecular mass, the planetary radius, the acceleration of gravity at the planet's surface, and the atmospheric density at the turbopause. The values for density, pressure, speed of sound, molecular mass, density scale height, number density, mean free path, and viscosity as functions of altitude are calculated with the mathematical relationships given in references 3 and 96; additional mathematical operations are required to determine the mean molecular mass values above the turbopause. All operations satisfy the hydrostatic equation and equation of state.

2.3.2 Choice of Model Parameters

Atmospheric models were computed for the lower and upper atmospheres to account for uncertainties in the atmospheric parameters. Table 4 shows the input parameters for the engineering models of the Venus atmosphere that have been developed. The lower atmosphere was based on temperature profiles determined from spacecraft measurements with surface values obtained by adiabatic extrapolation to the surface. Upper atmosphere models were calculated with the thermal model of reference 66 constrained at the lower boundary by values at the turbopause and at the upper boundary by exospheric temperatures. All models account for the variation of gravitational acceleration with altitude.

---

* $g_o = \dfrac{GM_{\varphi}}{r_o^2}$ where r_o is the planetary surface radius.

TABLE 4

COMPUTER INPUTS FOR MODELS OF VENUS ATMOSPHERE (1972)

Parameters	Model I (Most Probable Molecular Mass)	Models II, III, & VI (Maximum Molecular Mass)	Models IV & V (Minimum Molecular Mass)
Planetary Radius (km)	6050	6050*	6050**
Surface Gravity (cm/sec^2)	887.6	887.6	887.6
Surface Pressure (atm)	93.8	95.5*	86.7**
Surface Temperature (K)	767.5	772.5*	738.7**
Composition (% by volume)			
Below Turbopause			
CO_2	97	100	93
N_2	3	–	–
He	–	–	7
At Turbopause			
CO_2	95.99	100	93
N_2	3	–	–
He	0.01	–	5
O	1	–	2
Molecular Mass (g/g-mole)			
Below Turbopause	43.52	44.00	41.20
At Turbopause	43.24	44.00	41.44
Density at Turbopause (g/cm^3)	1.44×10^{-11}	1.46×10^{-13}	1.37×10^{-9}
Exospheric Temperature (K) (Model Number)			
Minimum Solar Activity	–	625 (II)	625 (IV)
Mean Solar Activity	710 (I)	–	–
Maximum Solar Activity	–	931 (III)	931 (V)
Night-Side Temperature	–	250 (VI)	–

*Extreme high values for surface pressure and temperature are obtained at a planetary radius of 6046 km (sec. 3.1).
**Extreme low values for surface pressure and temperature are obtained at a planetary radius of 6054 km (sec. 3.1).

2.3.2.1 Lower Atmosphere

The temperature profile for the lower atmosphere has been established by spacecraft measurements (fig. 10). A mean profile based on figure 10 is used for the most probable temperature profile and is shown in figure 16. The most probable model is computed for a planetary radius of 6050 km and a molecular mass of 43.5 determined for a composition of 97% CO_2 and 3% N_2. For all models of the lower atmosphere, it is assumed that the molecular mass is constant up to the turbopause.

Uncertainties in surface temperature and pressure are associated with topographic differences and uncertainties in composition. A range of values for local radii of 6046 to 6054 km was used, and two atmospheric compositions were chosen to encompass a reasonable range for molecular mass. One composition is pure CO_2 which provides the maximum molecular mass, and the other composition has 93% CO_2 and 7% He which provides the minimum molecular mass.

2.3.2.2 Upper Atmosphere

The lower boundary for the theoretical upper atmosphere is the turbopause. The turbopause is the altitude below which the atmospheric gases mix in constant proportions; above this altitude each constituent gas is taken to be in diffusive equilibrium, with number density decreasing with altitude at a rate which depends upon the molecular mass of the gas and the ambient atmospheric temperature. The turbopause was estimated for three possible values of eddy diffusion coefficient, 10^5, 10^7, and 10^9 cm^2/s which were selected to span a reasonable range of values. The coefficients then were used to determine the associated density values at the turbopause. The model of maximum molecular mass is a pure CO_2 atmosphere, the model of minimum molecular mass assumes the highest mixing ratios for O and He at the turbopause, and the model of most probable molecular mass was selected to give the most likely values of mixing ratios for O and He. The upper atmosphere models are superposed on the lower atmosphere models at the turbopause.

The upper constraint on the upper atmosphere models is the exospheric temperature which is a function of both diurnal heating and solar cycle heating. A value of 250K is for a night-side atmosphere with minimum solar activity. The temperatures presented in table 3 for minimum, mean, and maximum solar activity are used for day-side exospheric temperatures. The upper atmosphere temperature profiles for the different exospheric temperatures are shown in figure 16.

3. CRITERIA

The engineering models of the Venus atmosphere presented herein should be used for mission planning and design of space vehicles which are to orbit Venus, descend through the atmosphere, maneuver in the atmosphere, land on the planetary surface, or conduct scien-

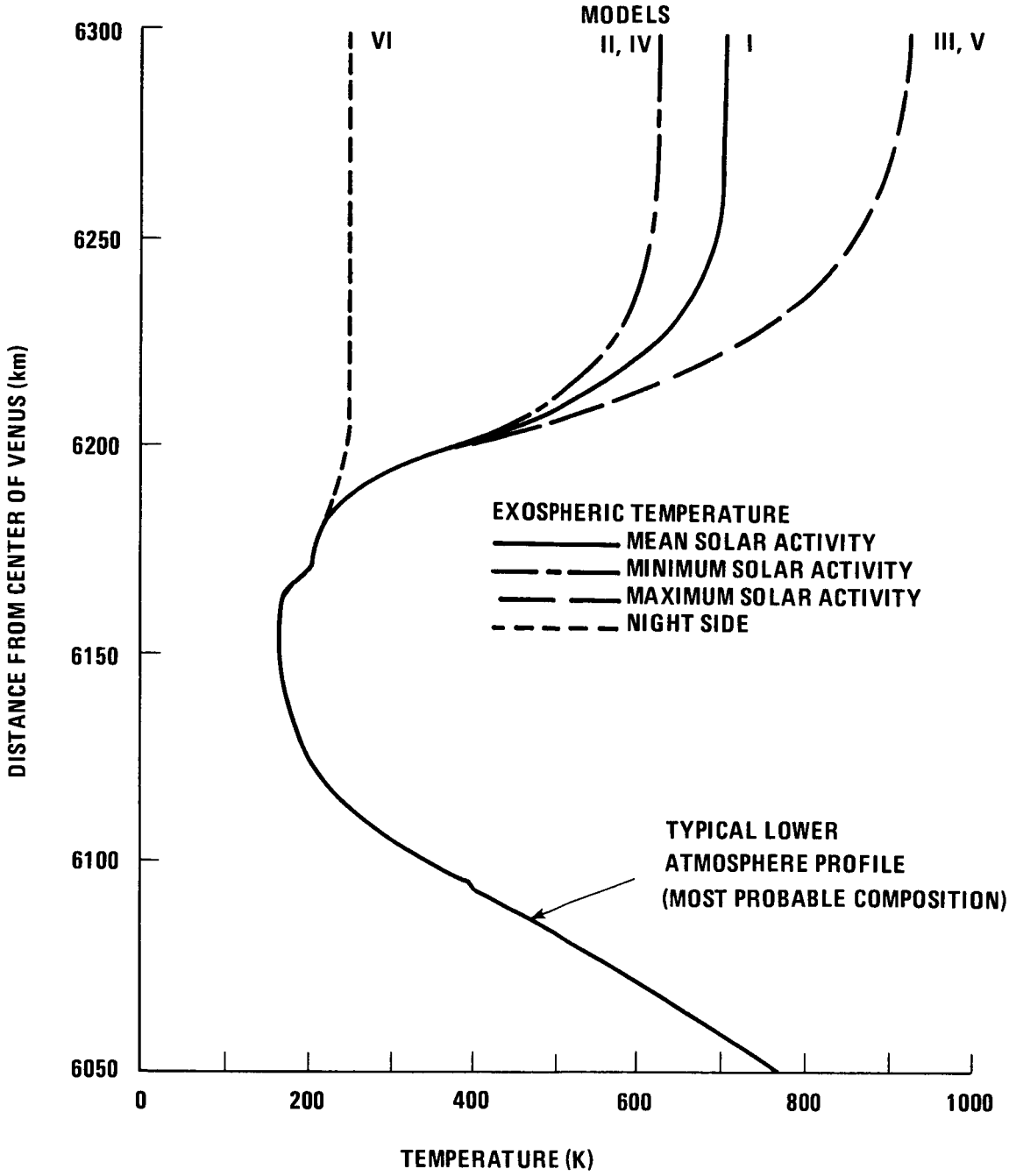

Figure 16.—Temperature profile for models of Venus atmosphere.

tific investigations during a planetary flyby mission. The models should be used for all facets of space vehicle design including

Structure
Deceleration system
Propulsion system
Flight control system
Guidance system
Heat shield and thermal control system
Communication systems
Electronics
Power supply
Mechanical devices
Scientific experiments (equipment and measurement ranges)

The models should be regarded as approximations which are based on the best available data and which encompass current uncertainties in the atmospheric parameters. The most probable model should be used as the nominal design model; it is most accurate in the lower atmosphere below an altitude of 70 km.

3.1 Atmospheric Models

The engineering models of the Venus atmosphere are given in tables 5 through 10. Model I (table 5) should be considered as the nominal model. Models II through VI (tables 6 through 10) take into account possible extremes of molecular mass, solar activity, and exospheric temperature in appropriate combinations as shown in table 4.

All models are based on the most probable planetary radius of 6050 km which corresponds to 0-km altitude in the tables. However, to encompass possible extremes of surface pressure and temperature, the tables have been extended downward to -4 km which corresponds to a planetary radius of 6046 km. Extreme high values for surface pressure and temperature should be read at -4 km in Models II, III, and VI (tables 6, 7, and 10). On the other hand, extreme low values for surface pressure and temperature should be read at +4 km in Models IV and V (tables 8 and 9) which corresponds to a planetary radius of 6054 km.

The six tables were terminated at altitudes where the density falls to 10^{-16} g/cm^3 because the hydrostatic equilibrium assumption upon which these models are based undoubtedly becomes invalid at greater altitudes.

An alternate model has been proposed in reference 99 which is generally consistent with the nominal model given in table 5. The alternate model is basically the one given in reference 63, but revised to reflect the surface temperature obtained from Venera 7. This model, however, does not incorporate the improved Mariner 5 results (ref. 49) which affect the model above 50 km.

3.2 Winds

Studies of the dynamics of the Venus atmosphere and limited data obtained from spacecraft indicate that the wind values presented in reference 3 are valid. Accordingly, the following wind parameter values should be used:

Mean horizontal wind speed below 50 km	2-30 m/sec
Mean horizontal wind speeds above 50 km	100 m/sec
Maximum wind shear	0.05 m/sec/m
Mean vertical wind speed	1 m/sec

3.3 Ionosphere

The theoretical thermal model of reference 65 should be used for computing the temperature and density of the ionosphere. The following peak values for electron density should be used:

Day Side	$5 \times 10^5/cm^3$
Night Side	$2 \times 10^4/cm^3$

3.4 Clouds

Two cloud layers have been identified, but cloud models are speculative. The following data for clouds have been proposed but should be regarded as tentative.

Cloud Layer	Altitude above Mean Surface (km)	Temperature (K)	Composition
Upper, or Haze	81 (top)	180	$HCl-H_2O$
Lower, Second, or Visible	60 (top)	260	Hg_2Cl_2
(not visible)	~ 53 (base)	~ 330	Hg
(not visible)	~ 51 (base)	~ 345	HgS
(not visible)	47 (base)	375	Hg_2I_2
(not visible)	44 (base)	400	Hg_2Br_2

Because wavelengths below 3 cm are severely attenuated, all communication wavelengths should be above 5 cm.

TABLE 5*

1972 VENUS ATMOSPHERE (MODEL I)

(MOST PROBABLE MOLECULAR MASS AND MEAN SOLAR ACTIVITY)

Altitude (km)	Temperature (K)	Pressure (mb)	Density (g/cm^3)	Speed of Sound (m/s)	Molecular Mass (g/g-mole)	Density Scale Height (km)	Number Density (per cm^3)	Mean Free Path (m)	Viscosity (kg/m·s)
-4	798.1	1.20+05	7.89-02	426.	43.531	20.52	1.09+21	1.33-09	3.33-05
0**	767.5	9.49+04	6.47-02	418.	43.531	19.79	8.95+20	1.62-09	3.24-05
4	736.5	7.41+04	5.27-02	410.	43.531	19.06	7.29+20	1.99-09	3.15-05
8	705.2	5.73+04	4.25-02	402.	43.531	18.32	5.88+20	2.46-09	3.06-05
12	673.4	4.38+04	3.40-02	393.	43.531	17.57	4.71+20	3.07-09	2.96-05
16	641.2	3.30+04	2.70-02	384.	43.531	16.81	3.73+20	3.88-09	2.85-05
20	608.5	2.46+04	2.11-02	375.	43.531	16.03	2.93+20	4.95-09	2.74-05
24	575.3	1.80+04	1.64-02	365.	43.531	15.24	2.27+20	6.39-09	2.62-05
28	541.4	1.29+04	1.25-02	355.	43.531	14.43	1.73+20	8.36-09	2.51-05
32	506.8	9.10+03	9.40-03	345.	43.531	13.59	1.30+20	1.11-08	2.39-05
36	471.4	6.25+03	6.94-03	334.	43.531	12.74	9.61+19	1.51-08	2.25-05
40	433.0	4.16+03	5.03-03	321.	43.531	11.82	6.97+19	2.08-08	2.09-05
44	397.6	2.67+03	3.52-03	308.	43.531	10.51	4.87+19	2.97-08	1.95-05
48	371.4	1.66+03	2.34-03	299.	43.531	9.19	3.23+19	4.47-08	1.82-05
52	336.8	9.91+02	1.54-03	286.	43.531	9.36	2.13+19	6.79-08	1.65-05
56	299.6	5.57+02	9.74-04	271.	43.531	7.99	1.35+19	1.07-07	1.49-05
60	267.6	2.93+02	5.72-04	258.	43.531	7.12	7.92+18	1.83-07	1.33-05
64	246.2	1.44+02	3.06-04	249.	43.531	6.13	4.24+18	3.42-07	1.23-05
68	231.9	6.71+01	1.51-04	242.	43.531	5.47	2.10+18	6.91-07	1.16-05
72	217.0	2.99+01	7.22-05	235.	43.531	5.30	9.99+17	1.45-06	1.10-05
76	200.4	1.25+01	3.27-05	227.	43.531	4.76	4.53+17	3.20-06	1.03-05
80	187.9	4.92+00	1.37-05	211.	43.531	4.46	1.90+17	7.63-06	.94-05
84	180.1	1.84+00	5.35-06	203.	43.531	4.16	7.40+16	1.95-05	.89-05
88	175.2	6.65-01	1.99-06	199.	43.531	3.97	2.75+16	5.27-05	.86-05
92	171.4	2.35-01	7.16-07	195.	43.531	3.88	9.91+15	1.46-04	.83-05
96	168.3	8.11-02	2.52-07	193.	43.531	3.77	3.49+15	4.15-04	.81-05
100	166.5	2.77-02	8.70-08	191.	43.531	3.74	1.20+15	1.20-03	.80-05
110	171.0	1.86-03	5.70-09	195.	43.531	3.70	7.88+13	1.84-02	.83-05
120	203.9	1.59-04	4.10-10	229.	43.531	4.09	5.67+12	2.55-01	1.04-05
130***	214.0	1.91-05	4.67-11	234.	43.531	4.75	6.46+11	2.24+00	1.09-05
140	268.0	3.01-06	5.81-12	261.	42.963	5.39	8.15+10	1.79+01	1.33-05
150	378.4	7.79-07	1.04-12	308.	42.015	6.92	1.49+10	9.76+01	1.85-05
160	502.4	2.98-07	2.91-13	355.	40.818	9.09	4.29+09	3.39+02	2.37-05
170	591.0	1.41-07	1.13-13	390.	39.404	11.62	1.73+09	8.40+02	2.67-05
180	641.4	7.51-08	5.32-14	414.	37.732	13.93	8.49+08	1.71+03	2.84-05
190	674.9	4.28-08	2.73-14	435.	35.781	15.66	4.60+08	3.16+03	2.96-05
200	691.5	2.58-08	1.50-14	455.	33.576	17.31	2.70+08	5.39+03	3.01-05
210	700.8	1.62-08	8.66-15	475.	31.179	18.70	1.67+08	8.70+03	3.04-05
220	705.5	1.06-08	5.18-15	496.	28.700	20.14	1.09+08	1.34+04	3.06-05
230	707.8	7.20-09	3.21-15	520.	26.266	21.71	7.37+07	1.97+04	3.06-05
240	709.0	5.07-09	2.06-15	544.	23.994	23.49	5.18+07	2.81+04	3.07-05
250	709.4	3.69-09	1.37-15	569.	21.963	25.54	3.76+07	3.87+04	3.07-05
260	709.4	2.75-09	9.43-16	593.	20.207	27.80	2.81+07	5.18+04	3.07-05
270	709.4	2.10-09	6.68-16	616.	18.719	30.21	2.15+07	6.77+04	3.07-05
280	709.4	1.64-09	4.86-16	638.	17.467	32.69	1.68+07	8.68+04	3.07-05
290	709.4	1.30-09	3.62-16	658.	16.409	35.15	1.33+07	1.10+05	3.07-05
300	709.4	1.05-09	2.75-16	677.	15.499	37.52	1.07+07	1.36+05	3.07-05
310	709.5	8.51-10	2.12-16	696.	14.699	39.74	8.69+06	1.67+05	3.07-05
320	709.5	7.01-10	1.66-16	713.	13.976	41.80	7.15+06	2.03+05	3.07-05
330	709.5	5.82-10	1.31-16	731.	13.306	43.71	5.95+06	2.45+05	3.07-05
340	709.5	4.89-10	1.05-16	749.	12.672	45.51	4.99+06	2.92+05	3.07-05
350	709.5	4.14-10	8.46-17	768.	12.063	47.24	4.22+06	3.44+05	3.07-05

*A one- or two-digit number (preceded by a plus or minus sign) following an entry indicates the power of ten by which that entry should be multiplied.

**Corresponds to planetary radius of 6050 km.

***Density is 1.44×10^{-11} g/cm^3 at the turbopause (lower boundary of upper atmosphere).

TABLE 6*

1972 VENUS ATMOSPHERE (MODEL II)

(MAXIMUM MOLECULAR MASS AND MINIMUM SOLAR ACTIVITY)

Altitude (km)	Temperature (K)	Pressure (mb)	Density (g/cm^3)	Speed of Sound (m/s)	Molecular Mass (g/g-mole)	Density Scale Height (km)	Number Density (per cm^3)	Mean Free Path (m)	Viscosity (kg/m·s)
-4	803.1	1.23+05	8.09-02	424.	44.010	20.39	1.11+21	1.30-09	3.34-05
0**	772.5	9.66+04	6.62-02	416.	44.011	19.65	9.06+20	1.59-09	3.25-05
4	741.5	7.54+04	5.38-02	408.	44.011	18.94	7.37+20	1.96-09	3.16-05
8	710.2	5.82+04	4.34-02	400.	44.011	18.21	5.94+20	2.43-09	3.07-05
12	678.5	4.45+04	3.47-02	392.	44.011	17.47	4.75+20	3.04-09	2.97-05
16	646.3	3.35+04	2.75-02	383.	44.011	16.72	3.76+20	3.84-09	2.86-05
20	613.7	2.49+04	2.15-02	374.	44.011	15.95	2.94+20	4.90-09	2.75-05
24	580.5	1.82+04	1.66-02	364.	44.011	15.17	2.28+20	6.34-09	2.64-05
28	546.7	1.31+04	1.27-02	355.	44.011	14.37	1.74+20	8.30-09	2.52-05
32	512.1	9.22+03	9.53-03	344.	44.011	13.54	1.30+20	1.11-08	2.40-05
36	476.6	6.33+03	7.03-03	333.	44.011	12.73	9.62+19	1.50-08	2.26-05
40	437.8	4.21+03	5.10-03	320.	44.011	11.82	6.97+19	2.07-08	2.10-05
44	402.0	2.71+03	3.56-03	308.	44.011	10.51	4.88+19	2.95-08	1.96-05
48	375.5	1.68+03	2.37-03	299.	44.011	9.20	3.24+19	4.45-08	1.83-05
52	340.5	1.00+03	1.56-03	286.	44.011	9.36	2.13+19	6.76-08	1.66-05
56	302.8	5.64+02	9.86-04	271.	44.011	8.00	1.35+19	1.07-07	1.49-05
60	270.3	2.96+02	5.80-04	258.	44.011	7.13	7.94+18	1.82-07	1.33-05
64	248.9	1.46+02	3.10-04	249.	44.011	6.12	4.24+18	3.40-07	1.23-05
68	234.5	6.79+01	1.53-04	242.	44.011	5.47	2.10+18	6.87-07	1.17-05
72	219.4	3.03+01	7.31-05	235.	44.011	5.31	1.00+18	1.44-06	1.10-05
76	202.6	1.27+01	3.31-05	227.	44.011	4.76	4.53+17	3.18-06	1.03-05
80	190.0	4.98+00	1.39-05	220.	44.011	4.46	1.90+17	7.59-06	.95-05
84	182.0	1.86+00	5.42-06	215.	44.011	4.16	7.41+16	1.94-05	.89-05
88	177.0	6.72-01	2.01-06	212.	44.011	3.96	2.75+16	5.24-05	.86-05
92	173.0	2.37-01	7.24-07	209.	44.011	3.88	9.91+15	1.45-04	.84-05
96	169.6	8.16-02	2.55-07	207.	44.011	3.76	3.49+15	4.14-04	.82-05
100	168.0	2.78-02	8.75-08	206.	44.011	3.73	1.20+15	1.20-03	.81-05
110	171.0	1.84-03	5.70-09	208.	44.011	3.68	7.79+13	1.85-02	.82-05
120	203.9	1.53-04	3.98-10	227.	44.011	4.05	5.45+12	2.64-01	1.04-05
130	214.0	1.79-05	4.44-11	232.	44.011	4.70	6.07+11	2.37+00	1.08-05
140	263.0	2.87-06	5.41-12	264.	41.210	5.41	7.90+10	1.82+01	1.30-05
150	366.6	7.48-07	1.01-12	306.	41.210	7.02	1.48+10	9.76+01	1.79-05
160***	471.9	2.74-07	2.88-13	343.	41.210	9.03	4.21+09	3.42+02	2.24-05
170	542.9	1.19-07	1.16-13	354.	44.011	10.53	1.59+09	9.09+02	2.51-05
180	583.8	5.41-08	4.90-14	366.	44.011	12.06	6.71+08	2.15+03	2.65-05
190	602.9	2.56-08	2.25-14	372.	44.011	13.09	3.08+08	4.68+03	2.71-05
200	612.7	1.24-08	1.07-14	374.	44.011	13.62	1.47+08	9.82+03	2.75-05
210	620.3	6.09-09	5.19-15	377.	44.011	13.90	7.11+07	2.03+04	2.77-05
220	620.8	3.00-09	2.56-15	377.	44.011	14.18	3.51+07	4.11+04	2.77-05
230	621.3	1.49-09	1.27-15	377.	44.011	14.23	1.73+07	8.31+04	2.77-05
240	621.5	7.38-10	6.29-16	377.	44.011	14.29	8.60+06	1.68+05	2.77-05
250	621.7	3.67-10	3.13-16	377.	44.011	14.34	4.28+06	3.37+05	2.78-05
260	621.7	1.83-10	1.56-16	377.	44.011	14.39	2.13+06	6.76+05	2.78-05
270	621.8	9.15-11	7.79-17	377.	44.011	14.44	1.07+06	1.35+06	2.78-05

*A one- or two-digit number (preceded by a plus or minus sign) following an entry indicates the power of ten by which that entry should be multiplied.

**Corresponds to planetary radius of 6050 km.

***Density is 1.46×10^{-13} g/cm^3 at the turbopause (lower boundary of upper atmosphere).

TABLE 7*

1972 VENUS ATMOSPHERE (MODEL III)

(MAXIMUM MOLECULAR MASS AND MAXIMUM SOLAR ACTIVITY)

Altitude (km)	Temperature (K)	Pressure (mb)	Density (g/cm^3)	Speed of Sound (m/s)	Molecular Mass (g/g-mole)	Density Scale Height (km)	Number Density (per cm^3)	Mean Free Path (m)	Viscosity (kg/m·s)
-4	803.1	1.23+05	8.09-02	424.	44.010	20.39	1.11+21	1.30-09	3.34-05
0**	772.5	9.66+04	6.62-02	416.	44.011	19.65	9.06+20	1.59-09	3.25-05
4	741.5	7.54+04	5.38-02	408.	44.011	18.94	7.37+20	1.96-09	3.16-05
8	710.2	5.82+04	4.34-02	400.	44.011	18.21	5.94+20	2.43-09	3.07-05
12	678.5	4.45+04	3.47-02	392.	44.011	17.47	4.75+20	3.04-09	2.97-05
16	646.3	3.35+04	2.75-02	383.	44.011	16.72	3.76+20	3.84-09	2.86-05
20	613.7	2.49+04	2.15-02	374.	44.011	15.95	2.94+20	4.90-09	2.75-05
24	580.5	1.82+04	1.66-02	364.	44.011	15.17	2.28+20	6.34-09	2.64-05
28	546.7	1.31+04	1.27-02	355.	44.011	14.37	1.74+20	8.30-09	2.52-05
32	512.1	9.22+03	9.53-03	344.	44.011	13.54	1.30+20	1.11-08	2.40-05
36	476.6	6.33+03	7.03-03	333.	44.011	12.73	9.62+19	1.50-08	2.26-05
40	437.8	4.21+03	5.10-03	320.	44.011	11.82	6.97+19	2.07-08	2.10-05
44	402.0	2.71+03	3.56-03	308.	44.011	10.51	4.88+19	2.95-08	1.96-05
48	375.5	1.68+03	2.37-03	299.	44.011	9.20	3.24+19	4.45-08	1.83-05
52	340.5	1.00+03	1.56-03	286.	44.011	9.36	2.13+19	6.76-08	1.66-05
56	302.8	5.64+02	9.86-04	271.	44.011	8.00	1.35+19	1.07-07	1.49-05
60	270.3	2.96+02	5.80-04	258.	44.011	7.13	7.94+18	1.82-07	1.33-05
64	248.9	1.46+02	3.10-04	249.	44.011	6.12	4.24+18	3.40-07	1.23-05
68	234.5	6.79+01	1.53-04	242.	44.011	5.47	2.10+18	6.87-07	1.17-05
72	219.4	3.03+01	7.31-05	235.	44.011	5.31	1.00+18	1.44-06	1.10-05
76	202.6	1.27+01	3.31-05	227.	44.011	4.76	4.53+17	3.18-06	1.03-05
80	190.0	4.98+00	1.39-05	220.	44.011	4.46	1.90+17	7.59-06	.95-05
84	182.0	1.86+00	5.42-06	215.	44.011	4.16	7.41+16	1.94-05	.89-05
88	177.0	6.72-01	2.01-06	212.	44.011	3.96	2.75+16	5.24-05	.86-05
92	173.0	2.37-01	7.24-07	209.	44.011	3.88	9.91+15	1.45-04	.84-05
96	169.6	8.16-02	2.55-07	207.	44.011	3.76	3.49+15	4.14-04	.82-05
100	168.0	2.78-02	8.75-08	206.	44.011	3.73	1.20+15	1.20-03	.81-05
110	171.0	1.84-03	5.70-09	208.	44.011	3.68	7.79+13	1.85-02	.82-05
120	203.9	1.53-04	3.98-10	227.	44.011	4.05	5.45+12	2.64-01	1.04-05
130	214.0	1.79-05	4.44-11	232.	44.011	4.70	6.07+11	2.37+00	1.08-05
140	272.3	2.80-06	5.44-12	259.	44.011	5.37	7.45+10	1.93+01	1.34-05
150	399.3	7.26-07	9.62-13	307.	44.011	6.95	1.32+10	1.10+02	1.95-05
160***	555.8	2.82-07	2.69-13	358.	44.011	9.23	3.68+09	3.92+02	2.55-05
170	675.4	1.37-07	1.07-13	392.	44.011	11.98	1.47+09	9.83+02	2.96-05
180	760.0	7.36-08	5.13-14	414.	44.011	14.41	7.01+08	2.05+03	3.21-05
190	826.0	4.21-08	2.70-14	431.	44.011	16.27	3.69+08	3.90+03	3.40-05
200	862.3	2.50-08	1.53-14	440.	44.011	18.10	2.10+08	6.87+03	3.51-05
210	890.2	1.51-08	9.00-15	447.	44.011	19.08	1.23+08	1.17+04	3.59-05
220	905.9	9.29-09	5.43-15	451.	44.011	19.99	7.43+07	1.94+04	3.64-05
230	916.7	5.75-09	3.32-15	453.	44.011	20.52	4.54+07	3.17+04	3.67-05
240	922.8	3.58-09	2.06-15	455.	44.011	20.94	2.81+07	5.13+04	3.68-05
250	926.8	2.24-09	1.28-15	455.	44.011	21.20	1.75+07	8.23+04	3.70-05
260	926.9	1.41-09	8.02-16	455.	44.011	21.46	1.10+07	1.31+05	3.70-05
270	926.9	8.82-10	5.04-16	456.	44.011	21.53	6.90+06	2.09+05	3.70-05
280	927.0	5.55-10	3.17-16	456.	44.011	21.60	4.34+06	3.32+05	3.70-05
290	927.1	3.50-10	2.00-16	456.	44.011	21.67	2.73+06	5.28+05	3.70-05
300	927.1	2.21-10	1.26-16	456.	44.011	21.74	1.72+06	8.37+05	3.70-05
310	927.2	1.39-10	7.95-17	456.	44.011	21.81	1.09+06	1.32+06	3.70-05

*A one- or two-digit number (preceded by a plus or minus sign) following an entry indicates the power of ten by which that entry should be multiplied.

**Corresponds to planetary radius of 6050 km.

***Density is 1.46×10^{-13} g/cm^3 at the turbopause (lower boundary of upper atmosphere).

TABLE 8*

1972 VENUS ATMOSPHERE (MODEL IV)

(MINIMUM MOLECULAR MASS AND MINIMUM SOLAR ACTIVITY)

Altitude (km)	Temperature (K)	Pressure (mb)	Density (g/cm^3)	Speed of Sound (m/s)	Molecular Mass (g/g-mole)	Density Scale Height (km)	Number Density (per cm^3)	Mean Free Path (m)	Viscosity (kg/m·s)
-4	768.9	1.11+05	7.14-02	431.	41.210	21.06	1.04+21	1.45-09	3.28-05
0**	738.7	8.77+04	5.89-02	423.	41.210	20.29	8.60+20	1.76-09	3.19-05
4	708.1	6.88+04	4.82-02	415.	41.210	19.53	7.04+20	2.15-09	3.10-05
8	677.1	5.34+04	3.91-02	406.	41.210	18.75	5.71+20	2.65-09	3.00-05
12	645.7	4.09+04	3.14-02	397.	41.210	17.96	4.59+20	3.30-09	2.89-05
16	613.9	3.10+04	2.50-02	388.	41.210	17.16	3.66+20	4.14-09	2.78-05
20	581.6	2.31+04	1.97-02	378.	41.210	16.34	2.88+20	5.25-09	2.67-05
24	548.7	1.70+04	1.53-02	368.	41.210	15.51	2.24+20	6.75-09	2.56-05
28	515.1	1.22+04	1.18-02	358.	41.210	14.65	1.72+20	8.80-09	2.44-05
32	480.9	8.62+03	8.89-03	347.	41.210	13.77	1.30+20	1.17-08	2.31-05
36	446.1	5.92+03	6.58-03	335.	41.210	12.81	9.61+19	1.58-08	2.16-05
40	409.8	3.94+03	4.77-03	322.	41.210	11.82	6.97+19	2.17-08	2.02-05
44	376.3	2.53+03	3.34-03	310.	41.210	10.51	4.87+19	3.11-08	1.86-05
48	351.5	1.57+03	2.21-03	301.	41.210	9.19	3.24+19	4.68-08	1.74-05
52	318.7	9.38+02	1.46-03	288.	41.210	9.36	2.13+19	7.10-08	1.58-05
56	283.5	5.27+02	9.22-04	273.	41.210	7.99	1.35+19	1.12-07	1.42-05
60	253.0	2.77+02	5.42-04	260.	41.210	7.12	7.92+18	1.91-07	1.27-05
64	233.0	1.36+02	2.90-04	251.	41.210	6.12	4.23+18	3.58-07	1.18-05
68	219.5	6.34+01	1.43-04	244.	41.210	5.46	2.09+18	7.24-07	1.12-05
72	206.4	2.83+01	6.80-05	237.	41.210	5.26	9.93+17	1.52-06	1.06-05
76	192.4	1.19+01	3.08-05	229.	41.210	4.81	4.50+17	3.37-06	.98-05
80	181.0	4.77+00	1.31-05	222.	41.210	4.52	1.91+17	7.94-06	.90-05
84	173.8	1.81+00	5.17-06	218.	41.210	4.24	7.56+16	2.00-05	.86-05
88	169.6	6.69-01	1.95-06	215.	41.210	4.04	2.86+16	5.30-05	.83-05
92	166.4	2.42-01	7.20-07	213.	41.210	3.97	1.05+16	1.44-04	.81-05
96	163.8	8.59-02	2.60-07	211.	41.210	3.86	3.80+15	3.99-04	.80-05
100	163.0	3.03-02	9.21-08	211.	41.210	3.85	1.35+15	1.13-03	.79-05
110***	171.0	2.27-03	6.57-09	216.	41.210	3.85	9.60+13	1.58-02	.84-05
120	203.9	2.24-04	5.23-10	241.	39.629	4.14	7.94+12	1.90-01	1.05-05
130	214.0	4.24-05	6.34-11	300.	26.595	5.24	1.44+12	1.05+00	1.10-05
140	263.0	1.88-05	1.06-11	483.	12.386	7.24	5.17+11	2.92+00	1.31-05
150	366.6	1.38-05	3.26-12	736.	7.179	11.82	2.73+11	5.52+00	1.80-05
160	471.9	1.19-05	1.69-12	937.	5.576	19.61	1.82+11	8.28+00	2.26-05
170	542.9	1.07-05	1.17-12	1062.	4.941	32.34	1.43+11	1.06+01	2.52-05
180	583.8	9.82-06	9.36-13	1134.	4.628	50.04	1.22+11	1.24+01	2.66-05
190	602.9	9.09-06	8.07-13	1174.	4.450	72.86	1.09+11	1.38+01	2.73-05
200	612.9	8.46-06	7.20-13	1198.	4.338	92.38	1.00+11	1.51+01	2.76-05
210	620.3	7.89-06	6.52-13	1216.	4.263	104.87	9.21+10	1.64+01	2.78-05
220	620.8	7.37-06	6.01-13	1224.	4.209	126.14	8.60+10	1.75+01	2.79-05
230	621.3	6.90-06	5.56-13	1230.	4.169	131.96	8.04+10	1.88+01	2.79-05
240	621.5	6.45-06	5.17-13	1235.	4.138	137.44	7.52+10	2.01+01	2.79-05
250	621.7	6.05-06	4.81-13	1239.	4.113	141.24	7,04+10	2.14+01	2.79-05
260	621.7	5.67-06	4.49-13	1242.	4.093	144.88	6.60+10	2.29+01	2.79-05
270	621.8	5.31-06	4.19-13	1244.	4.078	147.56	6.19+10	2.44+01	2.79-05
280	621.8	4.98-06	3.92-13	1246.	4.065	149.87	5.81+10	2.60+01	2.79-05
290	621.9	4.68-06	3.67-13	1248.	4.054	151.88	5.45+10	2.77+01	2.79-05
300	621.9	4.39-06	3.43-13	1249.	4.045	153.65	5.11+10	2.95+01	2.79-05
310	622.0	4.12-06	3.22-13	1251.	4.038	155.22	4.80+10	3.14+01	2.79-05
320	622.0	3.87-06	3.02-13	1252.	4.032	156.62	4.51+10	3.35+01	2.79-05
330	622.1	3.64-06	2.83-13	1252.	4.027	157.88	4.24+10	3.56+01	2.79-05

*A one- or two-digit number (preceded by a plus or minus sign) following an entry indicates the power of ten by which that entry should be multiplied.

**Corresponds to planetary radius of 6050 km.

***Density is 1.37×10^{-9} g/cm^3 at the turbopause (lower boundary of upper atmosphere).

TABLE 8* (CONTINUED)

Altitude (km)	Temperature (K)	Pressure (mb)	Density (g/cm^3)	Speed of Sound (m/s)	Molecular Mass (g/g-mole)	Density Scale Height (km)	Number Density (per cm^3)	Mean Free Path (m)	Viscosity (kg/m·s)
340	622.1	3.42-06	2.66-13	1253.	4.023	159.02	3.98+10	3.79+01	2.79-05
350	622.2	3.22-06	2.50-13	1254.	4.020	160.06	3.74+10	4.03+01	2.79-05
360	622.2	3.02-06	2.35-13	1254.	4.017	161.01	3.52+10	4.29+01	2.79-05
370	622.3	2.84-06	2.21-13	1254.	4.015	161.90	3.31+10	4.56+01	2.79-05
380	622.3	2.68-06	2.07-13	1255.	4.013	162.73	3.11+10	4.85+01	2.79-05
390	622.4	2.52-06	1.95-13	1255.	4.011	163.51	2.93+10	5.15+01	2.79-05
400	622.4	2.37-06	1.84-13	1255.	4.010	164.25	2.76+10	5.47+01	2.79-05
425	622.5	2.04-06	1.58-13	1256.	4.007	165.95	2.37+10	6.36+01	2.79-05
450	622.7	1.76-06	1.36-13	1256.	4.006	167.53	2.04+10	7.39+01	2.79-05
475	622.8	1.51-06	1.17-13	1256.	4.005	169.02	1.76+10	8.57+01	2.79-05
500	622.9	1.31-06	1.01-13	1257.	4.004	170.45	1.52+10	9.93+01	2.79-05
525	623.0	1.13-06	8.73-14	1257.	4.004	171.86	1.31+10	1.15+02	2.79-05
550	623.1	9.78-07	7.55-14	1257.	4.003	173.24	1.14+10	1.33+02	2.79-05
575	623.2	8.47-07	6.54-14	1257.	4.003	174.62	9.84+09	1.53+02	2.79-05
600	623.3	7.34-07	5.67-14	1257.	4.003	175.99	8.53+09	1.77+02	2.79-05
625	623.5	6.38-07	4.92-14	1257.	4.003	177.36	7.41+09	2.04+02	2.79-05
650	623.6	5.54-07	4.28-14	1257.	4.003	178.73	6.44+09	2.34+02	2.79-05
675	623.7	4.82-07	3.72-14	1258.	4.003	180.10	5.60+09	2.69+02	2.79-05
700	623.8	4.20-07	3.24-14	1258.	4.003	181.48	4.88+09	3.09+02	2.80-05
725	623.9	3.66-07	2.83-14	1258.	4.003	182.86	4.25+09	3.55+02	2.80-05
750	624.0	3.20-07	2.47-14	1258.	4.003	184.24	3.71+09	4.07+02	2.80-05
775	624.1	2.79-07	2.15-14	1258.	4.003	185.63	3.24+09	4.66+02	2.80-05
800	624.2	2.44-07	1.88-14	1258.	4.003	187.03	2.83+09	5.32+02	2.80-05
825	624.3	2.14-07	1.65-14	1258.	4.003	188.43	2.48+09	6.08+02	2.80-05
850	624.4	1.87-07	1.44-14	1258.	4.003	189.83	2.17+09	6.94+02	2.80-05
875	624.5	1.64-07	1.27-14	1258.	4.003	191.24	1.91+09	7.92+02	2.80-05
900	624.6	1.44-07	1.11-14	1259.	4.003	192.66	1.67+09	9.02+02	2.80-05
925	624.7	1.27-07	9.78-15	1259.	4.003	194.08	1.47+09	1.03+03	2.80-05
950	624.8	1.12-07	8.60-15	1259.	4.003	195.50	1.29+09	1.17+03	2.80-05
975	624.9	9.82-08	7.57-15	1259.	4.003	196.93	1.14+09	1.33+03	2.80-05
1000	627.1	8.66-08	6.65-15	1261.	4.003	170.30	1.00+09	1.51+03	2.81-05

*A one- to two-digit number (preceded by a plus or minus sign) following an entry indicates the power of ten by which that entry should be multiplied.

TABLE 9*

1972 VENUS ATMOSPHERE (MODEL V)

(MINIMUM MOLECULAR MASS AND MAXIMUM SOLAR ACTIVITY)

Altitude (km)	Temperature (K)	Pressure (mb)	Density (g/cm^3)	Speed of Sound (m/s)	Molecular Mass (g/g-mole)	Density Scale Height (km)	Number Density (per cm^3)	Mean Free Path (m)	Viscosity (kg/m·s)
-4	768.9	1.11+05	7.14-02	431.	41.210	21.06	1.04+21	1.45-09	3.28-05
0**	738.7	8.77+04	5.89-02	423.	41.210	20.29	8.60+20	1.76-09	3.19-05
4	708.1	6.88+04	4.82-02	415.	41.210	19.53	7.04+20	2.15-09	3.10-05
8	677.1	5.34+04	3.91-02	406.	41.210	18.75	5.71+20	2.65-09	3.00-05
12	645.7	4.09+04	3.14-02	397.	41.210	17.96	4.59+20	3.30-09	2.89-05
16	613.9	3.10+04	2.50-02	388.	41.210	17.16	3.66+20	4.14-09	2.78-05
20	581.6	2.31+04	1.97-02	378.	41.210	16.34	2.88+20	5.25-09	2.67-05
24	548.7	1.70+04	1.53-02	368.	41.210	15.51	2.24+20	6.75-09	2.56-05
28	515.1	1.22+04	1.18-02	358.	41.210	14.65	1.72+20	8.80-09	2.44-05
32	480.9	8.62+03	8.89-03	347.	41.210	13.77	1.30+20	1.17-08	2.31-05
36	446.1	5.92+03	6.58-03	335.	41.210	12.81	9.61+19	1.58-08	2.16-05
40	409.8	3.94+03	4.77-03	322.	41.210	11.82	6.97+19	2.17-08	2.02-05
44	376.3	2.53+03	3.34-03	310.	41.210	10.51	4.87+19	3.11-08	1.86-05
48	351.5	1.57+03	2.21-03	301.	41.210	9.19	3.24+19	4.68-08	1.74-05
52	318.7	9.38+02	1.46-03	288.	41.210	9.36	2.13+19	7.10-08	1.58-05
56	283.5	5.27+02	9.22-04	273.	41.210	7.99	1.35+19	1.12-07	1.42-05
60	253.0	2.77+02	5.42-04	260.	41.210	7.12	7.92+18	1.91-07	1.27-05
64	233.0	1.36+02	2.90-04	251.	41.210	6.12	4.23+18	3.58-07	1.18-05
68	219.5	6.34+01	1.43-04	244.	41.210	5.46	2.09+18	7.24-07	1.12-05
72	206.4	2.83+01	6.80-05	237.	41.210	5.26	9.93+17	1.52-06	1.06-05
76	192.4	1.19+01	3.08-05	229.	41.210	4.81	4.50+17	3.37-06	.98-05
80	181.0	4.77+00	1.31-05	222.	41.210	4.52	1.91+17	7.94-06	.90-05
84	173.8	1.81+00	5.17-06	218.	41.210	4.24	7.56+16	2.00-05	.86-05
88	169.6	6.69-01	1.95-06	215.	41.210	4.04	2.86+16	5.30-05	.83-05
92	166.4	2.42-01	7.20-07	213.	41.210	3.97	1.05+16	1.44-04	.81-05
96	163.8	8.59-02	2.60-07	211.	41.210	3.86	3.80+15	3.99-04	.80-05
100	163.0	3.03-02	9.21-08	211.	41.210	3.85	1.35+15	1.13-03	.79-05
110***	171.0	2.27-03	6.57-09	216.	41.210	3.85	9.60+13	1.58-02	.84-05
120	203.9	2.24-04	5.23-10	241.	39.629	4.14	7.94+12	1.90-01	1.05-05
130	214.0	4.24-05	6.34-11	300.	26.595	5.24	1.44+12	1.05+00	1.10-05
140	272.3	1.90-05	1.05-11	487.	12.570	7.27	5.05+11	2.99+00	1.36-05
150	399.3	1.41-05	3.17-12	750.	7.449	11.67	2.56+11	5.90+00	1.96-05
160	555.8	1.23-05	1.55-12	987.	5.841	18.20	1.60+11	9.45+00	2.57-05
170	675.4	1.12-05	1.03-12	1148.	5.180	29.21	1.20+11	1.26+01	2.97-05
180	760.0	1.04-05	7.99-13	1256.	4.836	43.66	9.95+10	1.52+01	3.23-05
190	826.0	9.83-06	6.63-13	1335.	4.631	58.36	8.62+10	1.75+01	3.41-05
200	862.3	9.31-06	5.84-13	1382.	4.497	83.96	7.82+10	1.93+01	3.52-05
210	890.2	8.85-06	5.27-13	1418.	4.403	101.14	7.20+10	2.09+01	3.60-05
220	905.9	8.44-06	4.85-13	1442.	4.334	126.91	6.74+10	2.24+01	3.64-05
230	916.7	8.05-06	4.52-13	1459.	4.281	144.98	6.36+10	2.37+01	3.68-05
240	922.8	7.69-06	4.25-13	1470.	4.240	164.51	6.04+10	2.50+01	3.69-05
250	926.8	7.35-06	4.01-13	1479.	4.207	177.86	5.74+10	2.63+01	3.70-05
260	926.9	7.03-06	3.81-13	1484.	4.179	198.55	5.49+10	2.75+01	3.70-05
270	926.9	6.73-06	3.63-13	1488.	4.156	203.88	5.26+10	2.87+01	3.70-05
280	927.0	6.44-06	3.46-13	1492.	4.137	208.52	5.03+10	3.00+01	3.70-05
290	927.1	6.17-06	3.30-13	1495.	4.120	212.61	4.82+10	3.13+01	3.71-05
300	927.1	5.91-06	3.15-13	1498.	4.106	216.26	4.61+10	3.27+01	3.71-05
310	927.2	5.66-06	3.00-13	1500.	4.093	219.53	4.42+10	3.41+01	3.71-05
320	927.2	5.42-06	2.87-13	1502.	4.082	222.51	4.24+10	3.56+01	3.71-05
330	927.3	5.20-06	2.75-13	1504.	4.073	225.22	4.06+10	3.72+01	3.71-05

*A one- or two-digit number (preceded by a plus or minus sign) following an entry indicates the power of ten by which that entry should be multiplied.

**Corresponds to planetary radius of 6050 km.

***Density is 1.37×10^{-9} g/cm^3 at the turbopause (lower boundary of upper atmosphere).

TABLE 9* (CONTINUED)

Altitude (km)	Temperature (K)	Pressure (mb)	Density (g/cm^3)	Speed of Sound (m/s)	Molecular Mass (g/g-mole)	Density Scale Height (km)	Number Density (per cm^3)	Mean Free Path (m)	Viscosity (kg/m·s)
340	927.4	4.99-06	2.63-13	1505.	4.065	227.71	3.89+10	3.88+01	3.71-05
350	927.4	4.78-06	2.52-13	1507.	4.057	230.01	3.73+10	4.04+01	3.71-05
360	927.5	4.59-06	2.41-13	1508.	4.051	232.14	3.58+10	4.21+01	3.71-05
370	927.5	4.40-06	2.31-13	1509.	4.046	234.12	3.44+10	4.39+01	3.71-05
380	927.6	4.22-06	2.21-13	1510.	4.041	235.97	3.30+10	4.58+01	3.71-05
390	927.7	4.05-06	2.12-13	1511.	4.036	237.71	3.16+10	4.77+01	3.71-05
400	927.7	3.89-06	2.03-13	1512.	4.033	239.34	3.04+10	4.97+01	3.71-05
425	927.9	3.51-06	1.83-13	1513.	4.025	243.04	2.74+10	5.50+01	3.71-05
450	928.0	3.18-06	1.66-13	1514.	4.019	246.32	2.48+10	6.08+01	3.71-05
475	928.2	2.88-06	1.50-13	1515.	4.015	249.27	2.24+10	6.72+01	3.71-05
500	928.3	2.61-06	1.35-13	1516.	4.012	251.98	2.03+10	7.42+01	3.71-05
525	928.5	2.36-06	1.23-13	1517.	4.010	254.52	1.84+10	8.19+01	3.71-05
550	928.6	2.14-06	1.11-13	1517.	4.008	256.93	1.67+10	9.03+01	3.71-05
575	928.7	1.95-06	1.01-13	1517.	4.007	259.24	1.52+10	9.94+01	3.71-05
600	928.9	1.77-06	9.18-14	1518.	4.006	261.48	1.38+10	1.09+02	3.71-05
625	929.0	1.61-06	8.34-14	1518.	4.005	263.68	1.25+10	1.20+02	3.71-05
650	929.2	1.46-06	7.59-14	1518.	4.005	265.83	1.14+10	1.32+02	3.71-05
675	929.3	1.33-06	6.91-14	1518.	4.004	267.96	1.04+10	1.45+02	3.71-05
700	929.4	1.22-06	6.30-14	1518.	4.004	270.08	9.47+09	1.59+02	3.71-05
725	929.6	1.11-06	5.74-14	1519.	4.004	272.18	8.64+09	1.75+02	3.71-05
750	929.7	1.01-06	5.24-14	1519.	4.004	274.28	7.89+09	1.91+02	3.71-05
775	929.9	9.24-07	4.79-14	1519.	4.003	276.38	7.20+09	2.10+02	3.71-05
800	930.0	8.45-07	4.37-14	1519.	4.003	278.47	6.58+09	2.29+02	3.71-05
825	930.1	7.73-07	4.00-14	1519.	4.003	280.57	6.02+09	2.51+02	3.71-05
850	930.2	7.07-07	3.66-14	1519.	4.003	282.67	5.51+09	2.74+02	3.71-05
875	930.4	6.48-07	3.35-14	1519.	4.003	284.77	5.04+09	2.99+02	3.71-05
900	930.5	5.93-07	3.07-14	1519.	4.003	286.88	4.62+09	3.27+02	3.72-05
925	930.6	5.44-07	2.82-14	1519.	4.003	288.99	4.24+09	3.56+02	3.72-05
950	930.8	4.99-07	2.58-14	1520.	4.003	291.12	3.89+09	3.88+02	3.72-05
975	930.9	4.58-07	2.37-14	1520.	4.003	293.24	3.57+09	4.23+02	3.72-05
1000	934.2	4.21-07	2.17-14	1522.	4.003	236.80	3.27+09	4.62+02	3.73-05

*A one- or two-digit number (preceded by a plus or minus sign) following an entry indicates the power of ten by which that entry should be multiplied.

TABLE 10*

1972 VENUS ATMOSPHERE (MODEL VI)

(MAXIMUM MOLECULAR MASS AND NIGHT-SIDE EXOSPHERIC TEMPERATURE)

Altitude (km)	Temperature (K)	Pressure (mb)	Density (g/cm^3)	Speed of Sound (m/s)	Molecular Mass (g/g-mole)	Density Scale Height (km)	Number Density (per cm^3)	Mean Free Path (m)	Viscosity (kg/m·s)
-4	803.1	1.23+05	8.09-02	424.	44.010	20.39	1.11+21	1.30-09	3.34-05
0**	772.5	9.66+04	6.62-02	416.	44.011	19.65	9.06+20	1.59-09	3.25-05
4	741.5	7.54+04	5.38-02	408.	44.011	18.94	7.37+20	1.96-09	3.16-05
8	710.2	5.82+04	4.34-02	400.	44.011	18.21	5.94+20	2.43-09	3.07-05
12	678.5	4.45+04	3.47-02	392.	44.011	17.47	4.75+20	3.04-09	2.97-05
16	646.3	3.35+04	2.75-02	383.	44.011	16.72	3.76+20	3.84-09	2.86-05
20	613.7	2.49+04	2.15-02	374.	44.011	15.95	2.94+20	4.90-09	2.75-05
24	580.5	1.82+04	1.66-02	364.	44.011	15.17	2.28+20	6.34-09	2.64-05
28	546.7	1.31+04	1.27-02	355.	44.011	14.37	1.74+20	8.30-09	2.52-05
32	512.1	9.22+03	9.53-03	344.	44.011	13.54	1.30+20	1.11-08	2.40-05
36	476.6	6.33+03	7.03-03	333.	44.011	12.73	9.62+19	1.50-08	2.26-05
40	437.8	4.21+03	5.10-03	320.	44.011	11.82	6.97+19	2.07-08	2.10-05
44	402.0	2.71+03	3.56-03	308.	44.011	10.51	4.88+19	2.95-08	1.96-05
48	375.5	1.68+03	2.37-03	299.	44.011	9.20	3.24+19	4.45-08	1.83-05
52	340.5	1.00+03	1.56-03	286.	44.011	9.36	2.13+19	6.76-08	1.66-05
56	302.8	5.64+02	9.86-04	271.	44.011	8.00	1.35+19	1.07-07	1.49-05
60	270.3	2.96+02	5.80-04	258.	44.011	7.13	7.94+18	1.82-07	1.33-05
64	248.9	1.46+02	3.10-04	249.	44.011	6.12	4.24+18	3.40-07	1.23-05
68	234.5	6.79+01	1.53-04	242.	44.011	5.47	2.10+18	6.87-07	1.17-05
72	219.4	3.03+01	7.31-05	235.	44.011	5.31	1.00+18	1.44-06	1.10-05
76	202.6	1.27+01	3.31-05	227.	44.011	4.76	4.53+17	3.18-06	1.03-05
80	190.0	4.98+00	1.39-05	220.	44.011	4.46	1.90+17	7.59-06	.95-05
84	182.0	1.86+00	5.42-06	215.	44.011	4.16	7.41+16	1.94-05	.89-05
88	177.0	6.72-01	2.01-06	212.	44.011	3.96	2.75+16	5.24-05	.86-05
92	173.0	2.37-01	7.24-07	209.	44.011	3.88	9.91+15	1.45-04	.84-05
96	169.6	8.16-02	2.55-07	207.	44.011	3.76	3.49+15	4.14-04	.82-05
100	168.0	2.78-02	8.75-08	206.	44.011	3.73	1.20+15	1.20-03	.81-05
110	171.0	1.84-03	5.70-09	208.	44.011	3.68	7.79+13	1.85-02	.82-05
120	203.9	1.53-04	3.98-10	227.	44.011	4.05	5.45+12	2.64-01	1.04-05
130	214.0	1.79-05	4.44-11	232.	44.011	4.70	6.07+11	2.37+00	1.08-05
140	232.0	2.39-06	5.45-12	241.	44.011	4.97	7.46+10	1.93+01	1.16-05
150***	239.0	3.56-07	7.89-13	244.	44.011	5.26	1.08+10	1.34+02	1.19-05
160	242.0	5.56-08	1.22-13	246.	44.011	5.39	1.66+09	8.66+02	1.20-05
170	245.0	8.94-09	1.93-14	247.	44.011	5.48	2.64+08	5.46+03	1.22-05
180	248.0	1.48-09	3.15-15	248.	44.011	5.56	4.31+07	3.34+04	1.23-05
190	249.0	2.49-10	5.29-16	249.	44.011	5.63	7.24+06	1.99+05	1.23-05
200	249.0	4.24-11	9.01-17	249.	44.011	5.66	1.23+06	1.17+06	1.23-05

*A one- or two-digit number (preceded by a plus or minus sign) following an entry indicates the power of ten by which that entry should be multiplied.

**Corresponds to planetary radius of 6050 km.

***Density is 1.46×10^{-13} g/cm^3 at the turbopause (lower boundary of upper atmosphere).

REFERENCES

1. Anon.: Planetary Explorer Phase A Report and Universal Bus Description. NASA Goddard Space Flight Center, May 1971.

2. Ingersoll, A. P.; and Leovy, C. B.: The Atmospheres of Mars and Venus. Annual Reviews of Astronomy and Astrophysics, vol. 9, 1971, pp. 147-182.

3. Anon.: Models of Venus Atmosphere (1968). NASA Space Vehicle Design Criteria (Environment), NASA SP-8011, Dec. 1968.

4. Opik, E.: The Aeolosphere and Atmosphere of Venus. Journal of Geophysical Research, vol. 66, no. 9, 1961.

5. Sagan, C.: The Radiation Balance of Venus. Jet Propulsion Laboratory, California Institute of Technology, TR 32-34, 1961.

6. Kaplan, L.: A Preliminary Model of the Venus Atmosphere. Jet Propulsion Laboratory, California Institute of Technology, TR 32-379, 1962.

7. Owen, R.: Theoretical Model Atmospheres of Venus. NASA TN D-2527, 1965.

8. Evans, D. E.; Pitts, D. E.; and Kraus, G. L.: Venus and Mars Nominal Natural Environment for Advanced Manned Planetary Mission Programs. NASA SP-3016, 1967.

9. Ross, F. E.: Photographs of Venus. Astron. J., vol. 67, 1928, pp. 57-92.

10. Koenig, L. R.; et al.: Handbook of the Physical Properties of the Planet Venus. NASA SP-3029, 1967.

11. de Vaucouleurs, G.; and Menzel, D. H.: Results of the Occultation of Regulus by Venus. Nature, vol. 188, Oct. 1960, pp. 28-33.

12. Menzel, D. H.; and de Vaucouleurs, G.: Final Report on the Occultation of Regulus by Venus, July 7, 1959. Air Force Cambridge Research Laboratory Report No. 227, 1961.

13. de Vaucouleurs, G.: Geometric and Photometric Parameters of the Terrestrial Planets. Icarus, vol. 3, no. 3, 1964, pp. 187-235.

14. Kuiper, G. P.: "On the Nature of the Venus Clouds," Planetary Atmospheres. IAU Symposium No. 40, Springer-Verlag (New York), 1971, pp. 91-109.

15. Connes, P.; Connes, J.; Benedict, W. S.; and Kaplan, L. D.: Traces of HCl and HF in the Atmosphere of Venus. Astrophysical Journal, vol. 147, March 1967, p. 1230.

16. Connes, P.; Connes, J.; Kaplan, L. D.; and Benedict, W. S.: Carbon Monoxide in the Venus Atmosphere. Astrophysical Journal, vol. 152, June 1968, p. 731.

17. Rea, D. G.: The Composition of the Upper Clouds of Venus. Reviews of Geophysics and Space Physics, vol. 10, no. 1, Feb. 1972, pp. 369-378.

18. Lyot, B.: Research on the Polarization of Light from Planets and Some Terrestrial Substances. NASA Report TT F-187, 1964.

19. Coffeen, D. L.: Wavelength Dependence of Polarization. Astron. J., vol. 74, 1969, pp. 446-460.

20. Hansen, J. E.; and Arking, A.: Clouds of Venus: Evidence for their Nature. Science, vol. 171, Feb. 19, 1971, pp. 669-672.

21. Sagan, C.; and Pollack, J. B.: On the Structure of the Venus Atmosphere. Icarus 10, 1969, pp. 274-289.

22. Ash, M. E.; et al.: The Case for the Radar Radius of Venus. J. of the Atmos. Sci., vol. 25, no. 4, July 1968, pp. 560-563.

23. Anderson, J. D.; et al.: The Radius of Venus as Determined by Planetary Radar and Mariner V Radio Tracking Data. J. of the Atmos. Sci., vol. 25, no. 6, Nov. 1968, pp. 1171-1174.

24. Campbell, D. B.; et. al.: Venus: Topography Revealed by Radar Data. Science, vol. 175, Feb. 4, 1972, pp. 514-516.

25. Clark, B. G.; and Kuzmin, A. D.: The Measurement of the Polarization and Brightness Distribution of Venus at 10.6-cm Wavelength. Astrophysical Journal, vol. 142, 1965, pp. 23-44.

26. Ash, M. E.; Shapiro, I. I.; and Smith, W. B.: Astronomical Constants and Planetary Ephemerides Deduced From Radar and Optical Observations. Astron. J., vol. 72, 1967, pp. 338-350.

27. Smith, W. B.; et al.: Surface-height Variations on Venus and Mercury. Radio Science, vol. 5, 1969, pp. 411-423.

28. Dickel, J. R.: 6-cm Observations and the Microwave Spectrum of Venus. Icarus 6, 1967, pp. 417-426.

29. Pollack, J. B.; and Morrison, D.: Venus: Determination of Atmospheric Parameters from the Microwave Spectrum. Icarus, 12, 1970, pp. 376-390.

30. Hall, R. W.; and Branson, N. F. B. A.: High Resolution Radio Observations of the Planet Venus at a Wavelength of 6 cm. Monthly Notes Royal Astronomical Society, 151, 1971, pp. 185-196.

31. Sinclair, A. C. E.; et al.: Preliminary Report on Interferometer Observations of Venus at 11.1 cm Wavelength. Radio Science, vol. 5, 1970, pp. 347-354.

32. Barath, E. T.; et. al.: Mariner II Microwave Radiometer Experiments and Results. Astron. J., vol. 69, no. 1, 1964, pp. 49-58.

33. Chase, S. C.; Kaplan, L. D.; and Neugebauer, G.: The Mariner II Infrared Radiometer Experiment. Journal of Geophysical Research, vol. 68, no. 22, 1963, pp. 6157-6169.

34. Avduevsky, V. S.; Marov, M. Ya.; and Rozhdestvensky, M. K.: Model of the Atmosphere of the Planet Venus Based on Results of Measurements Made by the Soviet Automatic Interplanetary Station Venera 4. Journal of the Atmospheric Sciences, vol. 25, no. 4, July 1968, pp. 537-545.

35. Kuzmin, A. D.; and Vetukhovskaya, Yu. N.: "Venera-4" and Interpretation of Radioastronomical Measurements of Venus. Cosmic Research, vol. 6, no. 4, July-August 1968, pp. 492-497.

36. Moroz, V. I.; and Kurt, V. G.: The Atmosphere of Venus (A Comparison of the Results of Astronomical Observations and Direct Experiment). Cosmic Research, vol. 6, no. 4, July-Aug. 1968, pp. 481-488.

37. Kuzmin, A. D.: The Atmosphere of Venus from Recent Investigations. Space Research IX, 11th Plenary Meeting of COSPAR, North-Holland Publishing Co. (Amsterdam), 1969, pp. 704-711.

38. Avduevsky, V. S.; Marov, M. Ya.; and Rozhdestvensky, M. K.: The Atmosphere of the Planet Venus from Data of the Soviet Space Probe Venera 4. Space Research IX, 11th Plenary Meeting of COSPAR, North-Holland Publishing Co. (Amsterdam), 1969, 745-759.

39. Avduevsky, V. S.; Marov, M. Ya; and Rozhdestvensky, M. K.: A Tentative Model of the Venus Atmosphere Based on the Measurements of Veneras 5 and 6. Journal of the Atmospheric Sciences, vol. 27, no. 4, July 1970, pp. 561-568.

40. Avduevsky, V. S.; Marov, M. Ya.; and Rozhdestvensky, M. K.: Results of Measurements Made on Venera 5 and Venera 6 Space Probes and a Model of the Venusian Atmosphere. Cosmic Research, vol. 8, no. 6, Nov.-Dec. 1970, pp. 800-808.

41. Kliore, A.; and Cain, D. L.: Mariner 5 and the Radius of Venus. Journal of the Atmospheric Sciences, vol. 25, no. 4, July 1968, pp. 549-554.

42. Avduevsky, V. S.; Marov, M. Ya.; and Rozhdestvensky, M. K.: Results of Measurement of Parameters of the Atmosphere of Venus by the Soviet Probe Venus 4. Cosmic Research, vol. 7, no. 2, March-April 1969, pp. 209-220.

43. Hunten, D. M.; and McElroy, M. B.: The Upper Atmosphere of Venus: The Regulus Occultation Reconsidered. Journal of Geophysical Research, vol. 73, no. 13, July 1, 1968, pp. 4446-4448.

44. Vinogradov, A. P.; Surkov, U. A.: and Florensky, C. P.: The Chemical Composition of the Venus Atmosphere Based on the Data of the Interplanetary Station Venera 4. Journal of the Atmospheric Sciences, vol. 25, no. 4, July 1968, pp. 535-536.

45. Vinogradov, A. P.; et. al.: The Chemical Composition of the Atmosphere of Venus. Planetary Atmospheres, IAU Symposium No. 40, Springer-Verlag (New York), 1971, pp. 3-16.

46. Mikhnevich, V. V.; and Sokolov, V. A.: A Model Atmosphere of Venus Based on the Results of Direct Temperature and Density Measurements. Cosmic Research, vol. 7, no. 2, March-April, 1969, pp. 197-208.

47. Mikhnevich, V. V.; and Sokolov, V. A.: Temperature and Density of the Venus Atmosphere According to Measurements Obtained by Venera 4. Space Research IX, 11th Plenary Meeting of COSPAR, North-Holland Publishing Co. (Amsterdam), 1969, pp. 730-744.

48. Kliore, A.; et. al.: Structure of the Atmosphere of Venus Derived from Mariner V S-Band Measurements. Space Research IX, 11th Plenary Meeting of COSPAR, North-Holland Publishing Co. (Amsterdam), 1969, 712-729.

49. Fjeldbo, G.; Kliore, A. J.; and Eshleman, V. R.: The Neutral Atmosphere of Venus as Studied with the Mariner V Radio Occultation Experiments. The Astronomical Journal, vol. 76, no. 2, March 1971, pp. 123-140.

50. Fjeldbo, G.; and Eshleman, V. R.: Atmosphere of Venus as Studied with the Mariner 5 Dual Radio-Frequency Occultation Experiment. Radio Science, vol. 4, no. 10, October 1969, pp. 879-897.

51. Barth, C. A.: Interpretation of the Mariner 5 Lyman Alpha Measurements. Journal of Atmospheric Sciences, 25, 1968, p. 564-567.

52. Barth, C. A.: Exospheric Temperature of Venus from Mariner 5. Planetary Atmospheres, IAU Symposium No. 40, Springer-Verlag (New York), 1971, pp. 17-22.

53. Kerzhanovich, V. V.; Andreev, B. N.; and Gotlib, V. M.: Investigation of the Dynamics of the Atmosphere of Venus with Automatic Interplanetary Stations Venera 5 and Venera 6. Soviet Physics-Doklady, vol. 15, no. 9, March 1971, pp. 797-799.

54. Kroupenio, N. N.: Peculiarities of mm and cm Radiowave Propogation in the Venus Atmosphere. Planetary Atmospheres, IAU Symposium No. 40, 1971, Springer-Verlag (New York), pp. 32-35.

55. Kolosov, M. A.; Yakovlev, O. I.; Yakovleva, G. P.; and Efimov, A. I.: Fluctuations of Radio Waves and Inhomogeneity of the Refractive Index of the Venusian Atmosphere. Cosmic Research, vol. 8, no. 6, Nov.-Dec. 1970, pp. 809-814.

56. Avduevsky, V. S.; Marov, M. Ya.; Rozhdestvensky, M. K.; Borodin, N. F.; and Kerzhanovich, V. V.: Soft Landing of Venera 7 on the Venus Surface and Preliminary Results of Investigations of the Venus Atmosphere. Journal of the Atmospheric Sciences, vol. 28, March 1971, pp. 263-269.

57. Belton, M. J. S.; and Hunten, D. M.: A Search for O_2 on Mars and Venus: A Possible Detection of Oxygen on Mars. Astrophys. J., vol. 153, 1968, pp. 963-974.

58. Avduevsky, V. S.; Marov, M. Ya.; Noykina, A. I.; Polezhaev, V. I.; and Zavelevich, F. S.: Heat Transfer in the Venus Atmosphere. Journal of the Atmospheric Sciences, vol. 27, no. 4, July 1970, pp. 569-579.

59. Lewis, J. S.: Venus: Atmospheric and Lithospheric Composition. Earth and Planetary Science Letters 10 (North-Holland Publishing Co.), 1970, pp. 73-80.

60. Lewis, J. S.: Geochemistry of the Volatile Elements on Venus. Icarus 11, 1969, pp. 367-385.

61. Lewis, J. S.: Ice Clouds on Venus? Journal of the Atmospheric Sciences, vol. 27, no. 2, March 1970, pp. 333-334.

62. Staley, D. O.: The Adiabatic Lapse Rate in the Venus Atmosphere. Journal of the Atmospheric Sciences, vol. 27, March 1970, pp. 219-223.

63. Marov, M. Ya.: A Model of the Atmosphere of Venus. Soviet Physics-Doklady, vol. 16, no. 1, July 1971, pp. 3-6.

64. Deirmendjian, D.: "Introductory Comments on Venus's Lower Atmosphere," The Atmospheres of Venus and Mars. Gordon and Breach Science Publishers, Inc. (New York), 1968, pp. 15-20.

65. McElroy, M. B.: The Upper Atmosphere of Venus. Journal of Geophysical Research, vol. 73, no. 5, March 1, 1968, pp. 1513-1521.

66. McElroy, M. B.: Ionization Processes in the Atmospheres of Venus and Mars. Annales de Geophysique, t. 26, fasc. 2, 1970, pp. 1-10.

67. Belton, M. J. S.: Planetary Atmospheres. EOS, Transactions American Geophysical Union, vol. 52, no. 6, June 1971, pp. IUGG 410-417.

68. Boyer, C.; and Camichel, H.: Observations Photographiques de la planète Vénus, Ann. d'Astrophys., 24, 1961, pp. 531-535.

69. Smith, B. A.: Rotations of Venus: Continuing Contradictions. Science, 152, 1967, pp. 114-116.

70. Schubert, G.; and Young, R. E.: The 4-Day Venus Circulation Driven by Periodic Thermal Forcing. Journal of Atmospheric Sciences, 27, 1970, pp. 523-528.

71. Guinot, B.; Mesures de la rotation de Vénus; Comptes Rendus. Académie des Sciences, Paris, 260, 1965, pp. 431-433.

72. Guinot, B.; and Feissel, M.: Mesure Spectrographique de Mouvements Dans L'Atmosphere de Vénus. Journal des Observateurs, vol. 51, 1968, pp. 13-20.

73. Malkus, W. V. R.: Hadley-Halley Circulation on Venus. Journal of Atmospheric Sciences, 27, 1970, pp. 529-533.

74. Schubert, G.: High Velocities Induced in a Fluid by a Traveling Thermal Source. Journal of Atmospheric Sciences, 26, 1969, pp. 767-770.

75. Schubert, G.; and Whitehead, J. A.: Moving Flame Experiment with Liquid Mercury: Possible Implication for the Venus Atmosphere. Science, 163, 1969, pp. 71-72.

76. Goody, R. M.; and Robinson, A. R.: A Discussion of the Deep Circulation of the Atmosphere of Venus. Astrophysical Journal, 146, 1966, pp. 339-355.

77. Stone, P. H.: Some Properties of Hadley Regimes on Rotating and Nonrotating Planets. Journal of Atmospheric Sciences, 25, 1968, pp. 644-657.

78. Zilitinkevich, S. S.; Monin, A. S.; Turikov, V. G.; and Chalikov, D. V.: Computer Simulation of the Circulation of the Atmosphere of Venus. Soviet Physics-Doklady, vol. 16, no. 4, Oct. 1971.

79. de Rivas, E. K.: Circulation of the Atmosphere of Venus. Ph.D. Thesis, MIT, 1971.

80. Barth, C. A.; Wallace, L.; and Pearce, J. B.: Mariner 5 Measurement of Lyman-Alpha Radiation Near Venus. J. Geophys. Res., vol. 73, 1968, pp. 2541-2545.

81. Kurt, V. G.; Dostovalow, S. B.; and Sheffer, E. K.: The Venus Far Ultraviolet Observations with Venera 4. Journal of the Atmospheric Sciences, vol. 25, no. 4, July 1968, pp. 668-671.

82. Barth, C. A.: Interpretation of the Mariner 5 Lyman Alpha Measurements. Journal of the Atmospheric Sciences, vol. 25, no. 4, July 1968, pp. 564-567.

83. McElroy, M. B.; and Hunten, D. M.: The Ratio of Deuterium to Hydrogen in the Venus Atmosphere. J. Geophys. Res., vol. 74, 1969, pp. 1720-1739.

84. Donahue, T. M.: Deuterium in the Upper Atmospheres of Venus and Earth. J. Geophys. Res, Space Physics, vol. 74, no. 5, March 1, 1969, pp. 1128-1137.

85. Herman, J. R.; Hartle, R. E.; and Bauer, S. J.: The Dayside Ionosphere of Venus. Planetary Space Science (Pergamon Press), vol. 19, 1971, pp. 443-460.

86. McElroy, M. B.; and Strobel, D. F.: Models for the Nightime Venus Ionosphere. J. Geophys. Res., Space Physics, vol. 74, no. 5, March 1, 1969, pp. 1118-1127.

87. Dickinson, R. E.: Circulation and Thermal Structure of the Venusian Thermosphere. Journal of the Atmospheric Sciences, vol. 28, no. 6, Sept. 1971, pp. 885-894.

88. Dessler, A. J.: "Ionizing Plasma Flux in the Martian Upper Atmosphere," In the Atmospheres of Venus and Mars. Gordon and Breach Science Publishers, Inc. (New York), 1968, pp. 241-250.

89. Bauer, S. J.; Hartle, R. E.; and Herman, J. R.: Topside Ionosphere of Venus and Its Interaction with the Solar Wind. Nature, vol. 225, 1970, pp. 533-534.

90. Cloutier, P. A.: Dynamics of the Interaction of the Solar Wind with a Planetary Atmosphere. Radio Science, vol. 5, no. 2, February 1970, pp. 387-389.

91. Banks, D. M.; and Axford, W. I.: Origin and Dynamical Behaviour of Thermal Protons in the Venusian Ionosphere. Nature, vol. 225, March 7, 1970, pp. 924-926.

92. Wallis, M. K.: Comet-Like Interaction of Venus with the Solar Wind, I. Cosmic Electrodynamics, vol. 3, no. 1, April 1972, pp. 45-49.

93. Lewis, J. S.: Refractive Index of Aqueous HCl Solutions and the Composition of the Venus Clouds. Nature, vol. 230, no. 5292, April 2, 1971, pp. 295-296.

94. Rasool, S. I.; and Stewart, R. W.: Results and Interpretation of the S-Band Occultation Experiments on Mars and Venus. Journal of the Atmospheric Sciences, vol. 28, no. 6, September 1971, pp. 869-878.

95. Anderson, E.: Mass and Dynamical Oblateness of Venus. American Astronomical Society Bulletin, vol. 1, no. 3, 1969, p. 231.

96. Pitts, D.: A Computer Program for Calculating Model Planetary Atmospheres. NASA TN D-4292, 1968.

97. Hilsenrath, J.: Tables of Thermodynamic and Transport Properties of Air, Argon, Carbon Dioxide, Carbon Monoxide, Nitrogen, Oxygen, and Steam. Pergamon Press (New York), 1960.

98. Brokaw, R. S.: Alignment Charts for Transport Properties, Viscosity, Thermal Conductivity, and Diffusion Coefficients for Non-polar Gases and Gas Mixtures at Low Density. NASA TR R-81, 1961.

99. Marov, M. Ya.: Venus: A Perspective at the Beginning of Planetary Exploration. Icarus, vol. 16, no. 3, June 1972, pp. 415-461.

NASA SPACE VEHICLE DESIGN CRITERIA MONOGRAPHS

ENVIRONMENT

SP-8005	Solar Electromagnetic Radiation, revised May 1971
SP-8010	Models of Mars Atmosphere (1967), May 1968
SP-8011	Models of Venus Atmosphere (1972), revised December 1972
SP-8013	Meteoroid Environment Model–1969 (Near Earth to Lunar Surface), March 1969
SP-8017	Magnetic Fields–Earth and Extraterrestrial, March 1969
SP-8020	Mars Surface Models (1968), May 1969
SP-8021	Models of Earth's Atmosphere (120 to 1000 km), May 1969
SP-8023	Lunar Surface Models, May 1969
SP-8037	Assessment and Control of Spacecraft Magnetic Fields, September 1970
SP-8038	Meteoroid Environment Model–1970 (Interplanetary and Planetary), October 1970
SP-8049	The Earth's Ionosphere, March 1971
SP-8067	Earth Albedo and Emitted Radiation, July 1971
SP-8069	The Planet Jupiter (1970), December 1971
SP-8084	Surface Atmospheric Extremes (Launch and Transportation Areas), May 1972
SP-8085	The Planet Mercury (1971), March 1972
SP-8091	The Planet Saturn (1970), June 1972
SP-8092	Assessment and Control of Spacecraft Electromagnetic Interference, June 1972
SP-8103	The Planets Uranus, Neptune, and Pluto (1971), December 1972.

STRUCTURES

SP-8001	Buffeting During Atmospheric Ascent, revised November 1970
SP-8002	Flight-Loads Measurements During Launch and Exit, December 1964

SP-8003	Flutter, Buzz, and Divergence, July 1964
SP-8004	Panel Flutter, July 1964
SP-8006	Local Steady Aerodynamic Loads During Launch and Exit, May 1965
SP-8007	Buckling of Thin-Walled Circular Cylinders, revised August 1968
SP-8008	Prelaunch Ground Wind Loads, November 1965
SP-8009	Propellant Slosh Loads, August 1968
SP-8012	Natural Vibration Modal Analysis, September 1968
SP-8014	Entry Thermal Protection, August 1968
SP-8019	Buckling of Thin-Walled Truncated Cones, September 1968
SP-8022	Staging Loads, February 1969
SP-8029	Aerodynamic and Rocket-Exhaust Heating During Launch and Ascent, May 1969
SP-8031	Slosh Suppression, May 1969
SP-8032	Buckling of Thin-Walled Doubly Curved Shells, August 1969
SP-8035	Wind Loads During Ascent, June 1970
SP-8040	Fracture Control of Metallic Pressure Vessels, May 1970
SP-8042	Meteoroid Damage Assessment, May 1970
SP-8043	Design–Development testing, May 1970
SP-8044	Qualification testing, May 1970
SP-8045	Acceptance testing, April 1970
SP-8046	Landing Impact Attenuation for Non-Surface-Planing Landers, April 1970
SP-8050	Structural Vibration Prediction, June 1970
SP-8053	Nuclear and Space Radiation Effects on Materials, June 1970
SP-8054	Space Radiation Protection, June 1970
SP-8055	Prevention of Coupled Structure-Propulsion Instability (Pogo), October 1970

SP-8056 Flight Separation Mechanisms, October 1970

SP-8057 Structural Design Criteria Applicable to a Space Shuttle, January 1971

SP-8060 Compartment Venting, November 1970

SP-8061 Interaction with Umblicals and Launch Stand, August 1970

SP-8062 Entry Gasdynamic Heating, January 1971

SP-8063 Lubrication, Friction, and Wear, June 1971

SP-8066 Deployable Aerodynamic Deceleration Systems, June 1971

SP-8068 Buckling Strength of Structural Plates, June 1971

SP-8072 Acoustic Loads Generated by the Propulsion System, June 1971

SP-8077 Transportation and Handling Loads, September 1971

SP-8079 Structural Interaction with Control Systems, November 1971

SP-8082 Stress-Corrosion Cracking in Metals, August 1971

SP-8083 Discontinuity stresses in Metallic Pressure Vessels, November 1971

SP-8095 Preliminary Criteria for the Fracture Control of Space Shuttle Structures, June 1971

GUIDANCE AND CONTROL

SP-8015 Guidance and Navigation for Entry Vehicles, November 1968

SP-8016 Effects of Structural Flexibility on Spacecraft Control Systems, April 1969

SP-8018 Spacecraft Magnetic Torques, March 1969

SP-8024 Spacecraft Gravitational Torques, May 1969

SP-8026 Spacecraft Star Trackers, July 1970

SP-8027 Spacecraft Radiation Torques, October 1969

SP-8028 Entry Vehicle Control, November 1969

SP-8033 Spacecraft Earth Horizon Sensors, December 1969

SP-8034 Spacecraft Mass Expulsion Torques, December 1969

SP-8036 Effects of Structural Flexibility on Launch Vehicle Control Systems, February 1970

SP-8047 Spacecraft Sun Sensors, June 1970

SP-8058 Spacecraft Aerodynamic Torques, January 1971

SP-8059 Spacecraft Attitude Control During Thrusting Maneuvers, February 1971

SP-8065 Tubular Spacecraft Booms (Extendible, Reel Stored), February 1971

SP-8070 Spaceborne Digital Computer Systems, March 1971

SP-8071 Passive Gravity-Gradient Libration Dampers, February 1971

SP-8074 Spacecraft Solar Cell Arrays, May 1971

SP-8078 Spaceborne Electronic Imaging Systems, June 1971

SP-8086 Space Vehicle Displays Design Criteria, March 1972

SP-8098 Effects of Structural Flexibility on Entry Vehicle Control Systems, June, 1972

CHEMICAL PROPULSION

SP-8025 Solid Rocket Motor Metal Cases, April 1970

SP-8039 Solid Rocket Motor Performance Analysis and Prediction, May 1971

SP-8041 Captive-Fired Testing of Solid Rocket Motors, March 1971

SP-8048 Liquid Rocket Engine Turbopump Bearings, March 1971

SP-8051 Solid Rocket Motor Igniters, March 1971

SP-8052 Liquid Rocket Engine Turbopump Inducers, May 1971

SP-8064 Solid Propellant Selection and Characterization, June 1971

NASA-Langley, 1972 —— 30